

HK-TN-91: HK LI Fibre Specifications

S. J. Jenkins, B. Bogdan, N. Foster, N. K. McCauley

July 2, 2025

Contents

5	0 Version log	2
6	1 Introduction	3
7	2 HK LI System Overview	3
8	3 Laser System Specification	5
9	4 Fibre Lab Measurements	6
10	4.1 Fibre Test Stand	7
11	4.2 Preliminary Measurements	7
12	4.3 Attenuation Measurements	10
13	4.4 Dispersion Measurements	12
14	4.5 Fibre Choice	13
15	5 Fibre Switching Device	14
16	5.1 Overview	14
17	5.2 General Comparisons	15
18	5.3 Cross-talk Measurements	16
19	5.4 Summary	17
20	6 Speed of Light Measurements	19
21	7 Fibre Length Requirements	20
22	7.1 Injector Cell Locations	22
23	7.2 Fibre Paths	24
24	8 Photon Yield Requirements	36
25	9 Summary	38
26	A Additional Cross Talk Plots	42
27	A.1 Weinert FP400URT	42
28	A.2 Weinert GIF50C	43

29 0 Version log

- 30 • v1 - First release of TN, circulated to HK UK calibration group for comments.
- 31 • v2 - Updated to reflect comments received from HK UK calibration group. Also updated
32 photon yield requirements due to identified bug in WCSim simulation. This is the first
33 version made available to the collaboration.
- 34 • v3 - Fibre length requirements altered after deciding on specific injector cell locations. No
35 longer requiring all fibres to be the same length. Full description of injector cell locations
36 and fibre lengths given, as well as updating the laser system diagram to provide attenuators
37 individually for laser heads.
- 38 • v3.1 - Minor revision to make it clearer that different lengths of fibre in the barrel is the
39 primary approach.

40 1 Introduction

41 The Hyper-Kamiokande experiment has a broad physics program, including the aim of making
 42 precision measurements of neutrino oscillation parameters. In order to make such precision mea-
 43 surements, a precise understanding of the detector itself is required. To this end an array of
 44 different calibration systems are planned, with each playing a crucial role in driving systematic
 45 uncertainties down to the percent-level required.

46 A key component of the calibration program is the light injection (LI) system, which has two
 47 primary aims. The first is to measure the optical properties of the water in the tank, and monitor
 48 how the measured absorption and scattering parameters evolve with time. The second is to provide
 49 light sources with which to calibrate PMT response. In order to illuminate the injectors, lengths
 50 of fibre optic cable will be used to carry light from the sources on the top of the tank, all the way
 51 to the injectors installed on the PMT support structure.

52 This technical note focuses on the fibre optic requirements for the LI system, describing the
 53 quantities and lengths of cables needed, along with the lab measurements performed to decide on
 54 which types of fibre optic cables to use.

55 2 HK LI System Overview

56 The HK LI system will be split into two parts, one for the inner detector (ID) and one for the
 57 outer detector (OD). The ID system will consist of 33 injector positions, each housing a diffuser
 58 and collimator. Full details of the diffuser and collimator designs and requirements can be found
 59 in HK-TN-0042 [1] and HK-TN-0065 [2], respectively. Of the ID injectors, 28 will be located in
 60 the barrel region, with 7 locations equally spaced in z , each having four positions equally spaced
 61 in θ . The bottom end-cap will feature four more injector locations, with the injectors all facing
 62 upwards in the $+z$ direction. The top end-cap will feature a single location, where a calibration
 63 port will be used, rather than fixing to the PMT support structure. Figure 1 shows the injector
 64 locations described. Installing injectors at different heights throughout the detector will allow
 65 water parameters to be measured as a function of depth.

66 The OD system will consist primarily of diffusers, using bare hemispheres coupled to fibres,
 67 rather than the housed versions used for the ID system; 122 of these OD diffusers will be installed.
 68 The current design features 84 equally spaced around the barrel region. This results in 7 rows
 69 of 12 diffusers, with rows alternately offset from one another. This configuration is particularly
 70 advantageous as it matches the number of rows in the ID system, simplifying the installation of
 71 the fibre optic cables. Each end-cap would then feature 19 diffusers, again equally spaced across
 72 the surface. A diagram showing this layout is presented in Figure 2. Finally, 12 collimators will be
 73 installed in the OD, in suitable locations to achieve long path lengths such as across the end caps
 74 and up the side of the barrel. These collimators will be exactly the same as those installed in the
 75 ID.

76 In order to illuminate the injectors, two separate systems will be employed. The first of these
 77 will be a system formed of either five or six picosecond pulsed laser sources, in the wavelength
 78 range 337-550 nm. This laser system will be used to illuminate all of the ID injectors, along
 79 with the 12 OD collimators. The OD diffusers on the other hand will be illuminated by an LED
 80 pulser system, utilising a series of 365 nm wavelength LEDs. Both of these systems will feature

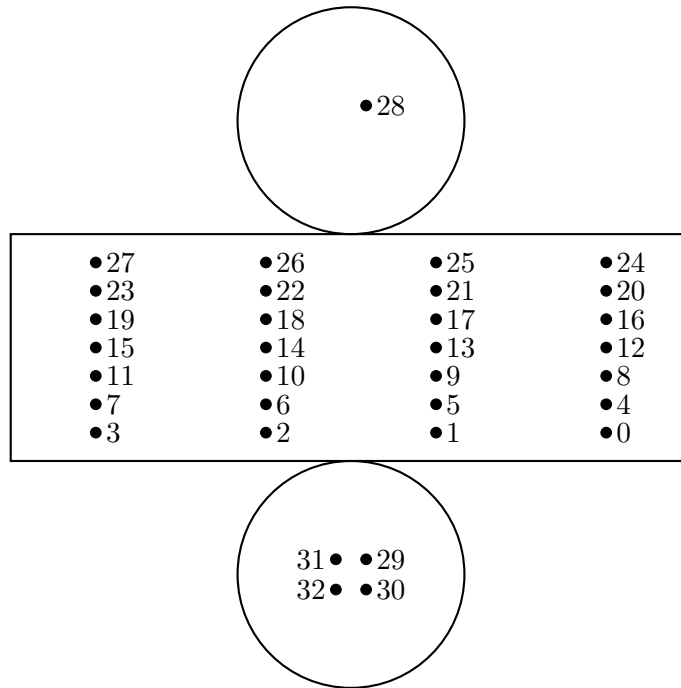


Figure 1: Injector location map for ID positions. Each location will feature a diffuser and collimator.

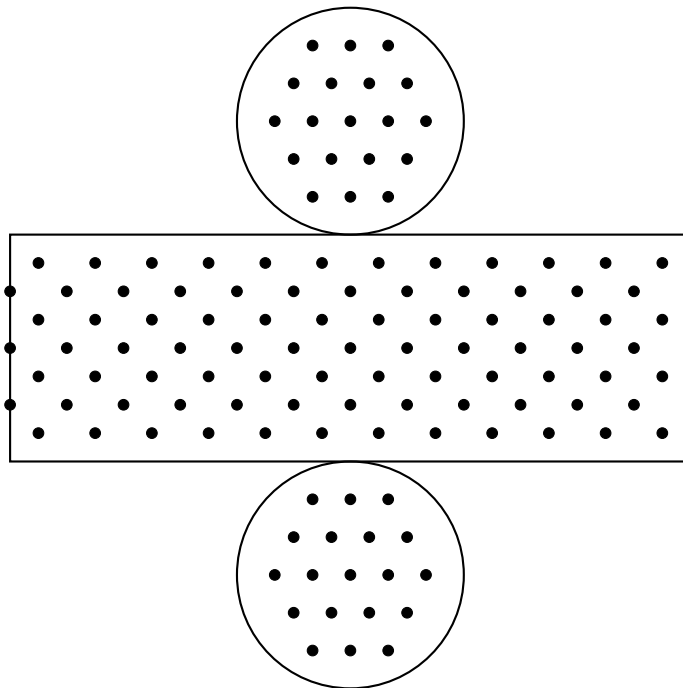


Figure 2: Injector location map for OD diffuser positions. Locations are approximate and dependent on PMT/WLS plate locations.

monitoring devices, so that the stability of the light sources can be monitored prior to convolution with detector parameters.

In total, including a laser diffuser ball and at least one spare channel, the lasers for the ID system will be required to couple to at least 80 channels. To accomplish this, dedicated fibre switching devices are required. A diagram giving an idea of the eventual laser and switch setup that would be used is given in Figure 3. These laser heads will be coupled into a single fibre using a 1-to-8

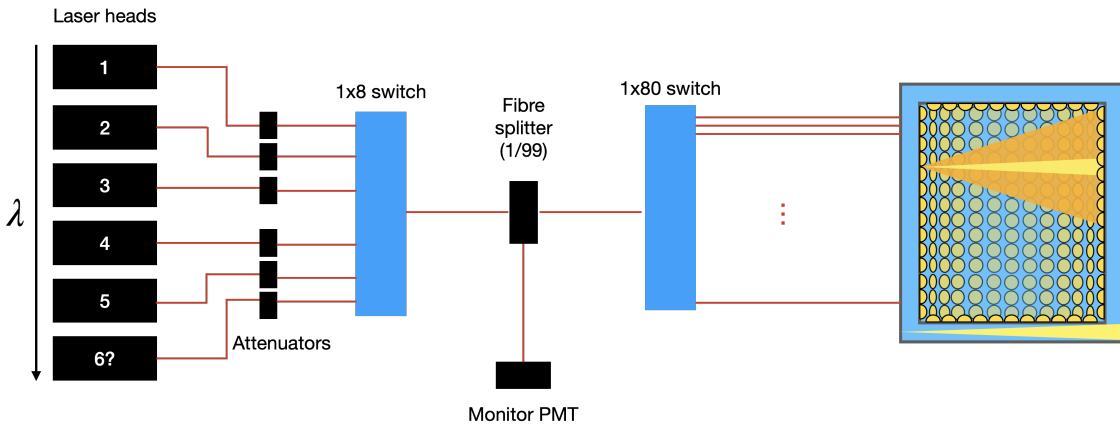


Figure 3: Diagram showing the likely setup for laser heads and fibre switchers.

(hereafter denoted as 1x8) switch, after each individually passing through air-gap attenuators. While only five laser heads are initially planned, this allows the system to be expanded at a later date if required. Individual attenuators are used so that the power can be manually tuned for each laser, independently of the others. The single fibre exiting the 1x8 switch can then connect to a fibre splitter with a 1/99 splitting. This allows 1% of the laser power to be directed to a nearby monitor PMT, which will monitor laser power before coupling into the long fibres and without entangling water parameters from within the detector. The fibre with the remaining 99% will go into a 1x80 switch, with the output going into the long fibres that extend down to the injectors.

3 Laser System Specification

In order to perform the desired calibrations across a range of wavelengths, a system of at least five pico-second diode lasers is required. These must ideally be controlled from a single unit, to simplify communication and operation during regular data-taking and dedicated calibration runs. These lasers should be fibre-coupled, to avoid the need to direct an open beam into the fibre system. Avoiding any open beams is also preferable in terms of safety to both users of the system, and any nearby workers. The intended setup for this laser system, as described in Section 2, is shown in Figure 3. While the setup will begin with five lasers heads, the switch will allow for up to eight to be connected, giving the ability to expand the system at a later date if required.

As the large lengths of fibre required to transport light from the laser sources to injection points will result in both attenuation and dispersion of the signal, output power and pulse width from the lasers should be maximised and minimised, respectively. The studies performed to estimate the required pulse energy to illuminate 1% of PMTs in spot region of each ID diffuser returned values of 5–10 pJ, with the maximum values at higher wavelengths. These studies are described in detail in Section 8. In certain scenarios, it will be necessary to inject more light into the detector than this. To account for this, a minimum pulse energy of 50 pJ was set for each laser wavelength. Coupling this with the requirement of short pulse widths, picosecond diode lasers were identified as the type of laser required. These lasers generally provide relatively high-powered pulses with pulse widths on the order of 1–100 ps.

Through our own market research and communicating with specialist laser suppliers, the pre-

ferred supplier identified for this system is PicoQuant [3], who manufacture high-powered pulsed picosecond diode lasers in a range of wavelengths. The Sepia PDL 828-L laser driver mainframe [4] allows for connection of up to eight laser drivers, which are all controlled from the single unit. This unit is capable of repetition frequencies with the internal oscillator of up to 80 MHz, though for the system in question triggering. The LDH Series of laser heads [5] provide pulses below 100 ps in length, in the wavelength range 375 to 1990 nm, with the option to run in pulsed or continuous mode. As an option, they can be fibre coupled, which as described will be necessary for the system. The laser heads which best fit the system requirements are the LDH-D-C-375, LDH-D-C-390, LDH-D-C-440 and LDH-D-C-500 [3], which provide peak wavelengths of 375 ± 5 , 395 ± 10 , 440 ± 10 and 500 ± 10 nm respectively. In order to go below 375 nm the LDH-FA Series of laser heads [6] can be used, which is a fibre amplified laser head, providing pulses of less than 80 ps in width. For this specific case, the LDH-P-FA-355 with peak wavelength at 355 ± 1 nm would be used. All of these laser heads fulfil the requirement of at least 50 pJ energy per pulse.

From this market research, it became clear that PicoQuant are the only company selling products that match the specification of both short pulse widths and high power. Several other companies which make picosecond diode lasers were contacted, but ultimately did not reach the power requirements. They are also fairly unique in the ability to control multiple laser heads with a single unit, whereas most commercial options need a single control unit per laser.

4 Fibre Lab Measurements

In order to make an informed decision on the optimal fibre optic cables to use for the LI system in HK, a series of measurements were made of the properties of the candidate fibres chosen. This section describes the fibre test stand setup at University of Liverpool, along with the measurements made of the candidate fibres, before discussing the decision on which fibres to use.

For the fibres to be suitable for use in the LI system, there are a series of requirements. These are:

- The fibre should be capable of transporting light of wavelengths in the range 337–550 nm.
- The attenuation of the input signal across the full length of fibre should be minimised.
- The dispersion of the input signal across the full length of fibre should be minimised.

Six different fibre types from Thorlabs were considered, to cover a range of options. Four of these were step-index fibres; two wide-core fibres (FP200URT [7] and FP400URT [8]) and two narrow-core fibres (FG050UGA [9] and FG105UCA [10]) were chosen. The remaining two candidates were graded-index fibres (GIF50C [11] and GIF50D [12]). Graded-index fibres were tested as it was expected that they would be required to limit dispersion of input signals across the full fibre length. It was particularly important to test the graded-index fibres as they are primarily for communications applications, and as such are only specified for operation above 800 nm. The main specifications of each fibre type are summarised in Table I. GIF50C and GIF50D have almost the same specifications, with the only difference being the available bandwidth. Preliminary measurements were performed with all six fibre types listed, and these results were used to make an informed choice on which should be investigated more thoroughly.

Fibre	Type	Core ϕ [μm]	NA	Transmission region [nm]
FG050UGA	Step-index	50	0.22	250-1200
FG105UCA	Step-index	105	0.22	250-1200
FP200URT	Step-index	200	0.50	300-1200
FP400URT	Step-index	400	0.50	300-1200
GIF50C	Graded-index	50	0.20	800-1600
GIF50D	Graded-index	50	0.20	800-1600

Table I: Fibre types used for initial testing in lengths of 1 m and 35 m.

4.1 Fibre Test Stand

All fibre measurements were performed using the fibre test stand in the Particle Physics Optical Laboratory at the University of Liverpool. Two different types of light sources are available for testing; the first of these is a Picoquant Sepia PDL 828-L laser driver [4], powering a LDH-D-C-375M laser head [5], with a peak wavelength of 371 nm. This is a pulsed laser source with a pulse width of \sim 50 ps, and repetition rate up to 80 MHz. The candidate fibres couple directly to the laser head using an FC/PC connector. The second set of light sources was a series of LEDs, covering wavelengths from 365 nm up to 595 nm. These are run in DC mode, and were used primarily to make attenuation measurements over the range of wavelengths relevant for the LI system. In order to connect the FC/PC connector on a candidate fibre to a surface-mounted LED, custom connectors were 3D printed.

Two different detection methods for the fibre transmitted light are available. To measure power output, a Thorlabs PM100USB [13] power meter is used, with an S150C sensor [14] connected. For timing measurements, the fibres are connected to a Hamamatsu H10721-210 PMT [15], which is read out by a Tektronix MSO54 oscilloscope [16]. Fibres are coupled to either read-out method via FC/PC connection such that, in the case of the laser, there are no bare beams in the lab. To ensure light tightness and as an additional safety measure, all light sources and detectors are housed within a dark box, with no connections made outside. Larger fibre reels are kept outside due to their size, with a port used to bring the ends inside for connection. An image of the setup is shown in Figure 4.

4.2 Preliminary Measurements

In order to narrow down the choice of fibre optic cable, all six options listed in Table I were purchased, in lengths of 1 m and 35 m. This is much shorter than the fibres that will be needed for Hyper-K; full length fibres were not used due to supplier issues. The length of cables which could be cut was limited by the size of the building used for production, as cold weather conditions during winter in the US at the time of ordering prevented them from being cut outside. Rather than delay the measurements, the decision was taken to start preliminary measurements of attenuation and dispersion with the lengths that were available.

4.2.1 Testing

Due to the early stage at which these measurements were made, the laser module described in Section 4.1 had not yet been set up. Instead, preliminary measurements of both attenuation and

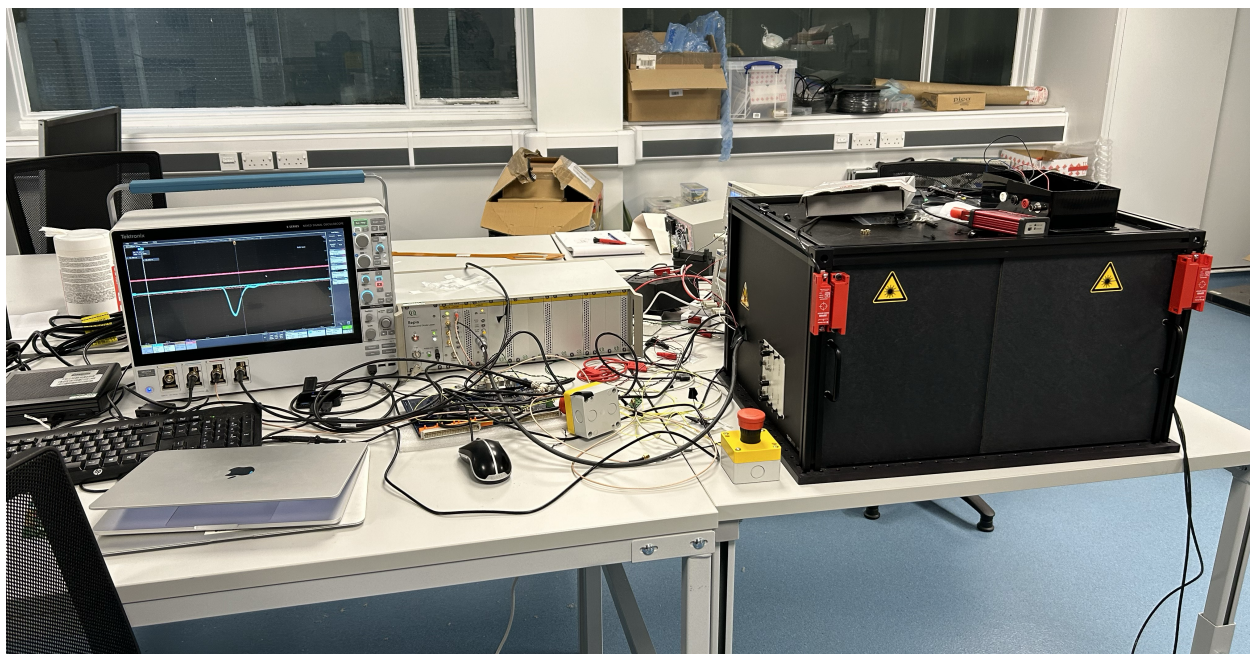


Figure 4: Fibre test stand in the optical lab at University of Liverpool.

dispersion were made using a pulsed 385 nm LED, operated by an early design of the LED pulser board that will be used for the OD LED system. In all tests, the 35 m lengths of fibre were left on the reels. This was both to remove cladding modes, as well as just to simplify the tests and not have to unwind this length of fibre around the lab. The 1 m fibres were also coiled to remove cladding modes as much as possible, though with such a short length the amount this could be done was limited.

To calculate dispersion of the signal across the fibre length, the width of the PMT signal pulse was measured for both lengths of each fibre. The pulse width is defined as the time elapsed while the voltage is at greater than 50% of the peak. A total of 20,000 measurements were made for each set to estimate the uncertainty. Subtracting these values in quadrature obtains the amount of dispersion observed. The pulse widths at both lengths and calculated dispersion values for each fibre are presented in Table II. The results shown here are mostly unsurprising. As expected, the

Fibre	Pulse width at 1 m [ns]	Pulse width at 35 m [ns]	Dispersion [ns]
FG050UGA	3.486 ± 0.111	4.207 ± 0.305	2.355 ± 0.569
FG105UCA	3.734 ± 0.075	4.841 ± 0.205	3.081 ± 0.335
FP200URT	3.809 ± 0.045	5.117 ± 0.158	3.416 ± 0.242
FP400URT	4.329 ± 0.054	5.252 ± 0.116	2.974 ± 0.219
GIF50C	3.453 ± 0.103	3.867 ± 0.260	1.741 ± 0.613
GIF50D	3.407 ± 0.101	3.899 ± 0.213	1.896 ± 0.509

Table II: Pulse width and dispersion values for initial fibre measurements, using a 385 nm pulsed LED source.

two graded-index fibres show the smallest amount of dispersion; this is exactly the reason they were added for consideration. For the first three step-index fibres, the dispersion increases with increased core diameter. However, it can be seen that the FP400URT, which has the largest core diameter, actually has a smaller amount of dispersion than the FP200URT. The typical rise time

201 of a 50 cm PMT is quoted to be 5 ns [17], so the fact that the pulse widths for all fibres but
 202 FP400URT are below this is a good sign.

203 The same set-up was also used to make preliminary measurements of attenuation in the fibres.
 204 As this was an early version of the fibre test stand, an optical power meter was not used. Instead,
 205 the area under the curve of each recorded pulse was used as a proxy, as this is proportional to the
 206 total charge collected by the PMT per pulse. Again, 20,000 measurements for each fibre sample
 were taken, and the results for this are presented in Table III. Again, the results shown here

Fibre	1 m [nVs]	35 m [nVs]	Transmittance [%]
FG050UGA	1.86 ± 0.23	0.75 ± 0.23	40.3 ± 13.3
FG105UCA	7.16 ± 0.62	4.17 ± 0.28	58.2 ± 6.4
FP200URT	16.53 ± 0.99	9.59 ± 0.74	58.0 ± 5.7
FP400URT	23.56 ± 1.14	19.24 ± 0.94	81.7 ± 5.6
GIF50C	4.61 ± 0.69	4.09 ± 0.59	88.7 ± 18.4
GIF50D	2.39 ± 0.57	0.56 ± 0.24	23.4 ± 11.5

Table III: Area-under-curve measurements from oscilloscope for 1 m and 35 m fibres, with calculated transmittance values.

207
 208 are unsurprising for the step-index fibres, with the transmittance increasing with increased core
 209 diameter. It can also be seen that the recorded values through the 1 m patch cable increase with
 210 increasing core diameter; this shows the difficulty of coupling particularly narrow-core fibres to an
 211 LED, which generally have a wide opening-angle for the light profile. The results obtained for the
 212 two graded-index fibres are seen to be very different, which is potentially related to the different
 213 bandwidths they're designed for, and the fact they're not specified for a wavelength range below
 214 800 nm. The amount of charge collected from a 1 m fibre for either of these types is again small
 215 due to them having a 50 μm core diameter, and suggests as expected that narrow-core fibres are
 216 not suitable for the OD LED pulser system.

217 4.2.2 Results

218 The results from these initial tests suggest that different fibre types will need to be employed for
 219 the ID laser and OD LED systems. For the OD LED system, where coupling the fibre to the LED
 220 and maximising light transmission is important, a wide-core fibre should likely be chosen. The
 221 FP400URT fibre showed the best transmission and input light acceptance, so this is the candidate
 222 that was favoured. For the laser system timing is more important; the dispersion measurements
 223 suggested that the graded-index GIF50C and GIF50D fibres were the best candidates here.

224 As this was a preliminary version of the fibre test stand, and measurements were carried out
 225 with fibre lengths significantly shorter than what will actually be installed into Hyper-K, the
 226 decision was initially taken to purchase three candidate fibres for further testing. These were
 227 FP400URT, GIF50C and GIF50D. Based on estimates of the length required, reels of 40 m and
 228 105 m length were purchased for each of these fibre types. However, it was later understood that
 229 the feed-throughs for the injectors would use an FG105UCA patch cable. In order to not add extra
 230 inefficiencies to the system in coupling different fibres to one another, the ideal scenario would
 231 be to use this fibre for the laser system. A reel of 105 m for this was also purchased and tested,
 232 with results for all four primary candidate fibres described together in the following sections for

233 simplicity.

234 **4.3 Attenuation Measurements**

235 **4.3.1 Method**

236 The full laser setup for the HK LI system will feature a minimum of five laser heads, over a range
 237 of wavelengths spanning UV to visible. In order to confirm whether attenuation in the candidate
 238 fibres is of an acceptable level across multiple wavelengths, LEDs across a series of wavelengths
 239 were used for these tests. Those were: 365, 395, 415, 465, 496, 525 and 560 nm. As timing is not
 240 relevant to attenuation measurements, and to ensure results were valid by initially getting enough
 241 light into the fibres, these LEDs were powered with a DC source.

242 Measurements were made of the output power from fibres of length 1, 2, 37, 42, 77, 107 and
 243 147 m, where some of these lengths were formed by coupling together multiple fibres of shorter
 244 length, and all lengths above 1 m featured two 1 m patch cables in the setup. To connect fibres
 245 together, FC/PC to FC/PC mating sleeves were used, which are quoted to have < 0.5 dB insertion
 246 loss [18]. As a 40 m length of FG105UCA fibre was not ordered, the measurements for this were
 247 done at slightly altered lengths. Power measurements were made using an optical power meter,
 248 as described in Section 4.1. The longer reels of fibre were purchased without tubing, and it was
 249 observed during data taking that there was some level of light leakage into the fibres, causing
 250 non-zero readings when the LEDs were not powered. To mitigate this, all measurements were
 251 performed with the reels of fibre that were too big to fit inside the dark box wrapped in black
 252 sheet.

253 The power observed after transmission through a fibre of length x can be written as

$$254 P = P_0 \exp^{-\lambda x}, \quad (1)$$

255 where P is the observed power after traversing the fibre, P_0 is the initial power, and λ is the
 256 coefficient of attenuation, describing how much attenuation occurs per unit length. Taking the
 257 natural logarithm of this,

$$258 \ln P = -\lambda x + \ln P_0, \quad (2)$$

259 allows a linear fit to be made to data, where the gradient is the coefficient of attenuation, and
 260 the y-intercept the log of the input power. The fitted attenuation coefficient can then be used to
 261 calculate attenuation in dB for a given fibre length, where in this case a length of 150 m is used:

$$262 \text{Attenuation (dB/150 m)} = \frac{10}{\ln 10} \times 150 \times \lambda. \quad (3)$$

263 **4.3.2 Results**

264 As a first check of the measurement system, the calculated attenuation values for the FP400URT
 265 fibre were compared to those provided in the fibre specifications by Thorlabs. This comparison can
 266 be seen in Figure 5, and shows generally good agreement between the two. Values of attenuation
 267 stay below 10 dB until just above 400 nm, where the amount of attenuation increases sharply.
 268 At the minimum wavelength of 365 nm, attenuation of over 20 dB is observed, suggesting that

269 attenuation values in the UV range will likely be the driving factor for deciding on a fibre type.

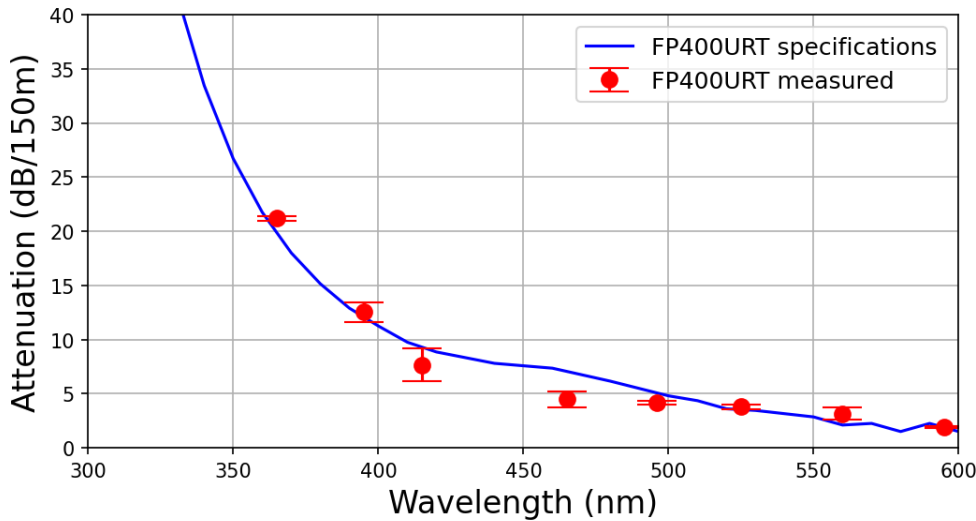


Figure 5: Measured attenuation scaled to 150 m length as a function of wavelength for the FP400URT fibre, compared to specifications from Thorlabs [8].

270 The full results for all fibre types are presented in Figure 6, with all values of attenuation again
 271 scaled to what would be seen across 150 m of fibre. As was shown for the FP400URT fibre, the
 272 amount of attenuation observed in the fibres peaks at the lowest wavelength scanned, 365 nm. At
 273 this value there is a large range of values observed, with the FG105UCA fibre exhibiting the lowest
 274 attenuation at under 15 dB. Conversely, the two graded index fibres show much greater attenuation.
 275 The spread of values at 395 nm is much reduced, with the two graded-index fibres instead exhibiting
 276 lower attenuation here. Above 400 nm, the FG105UCA fibre is seen to consistently exhibit higher
 attenuation than the other fibres, though in all cases is still below 10 dB. These results suggest that

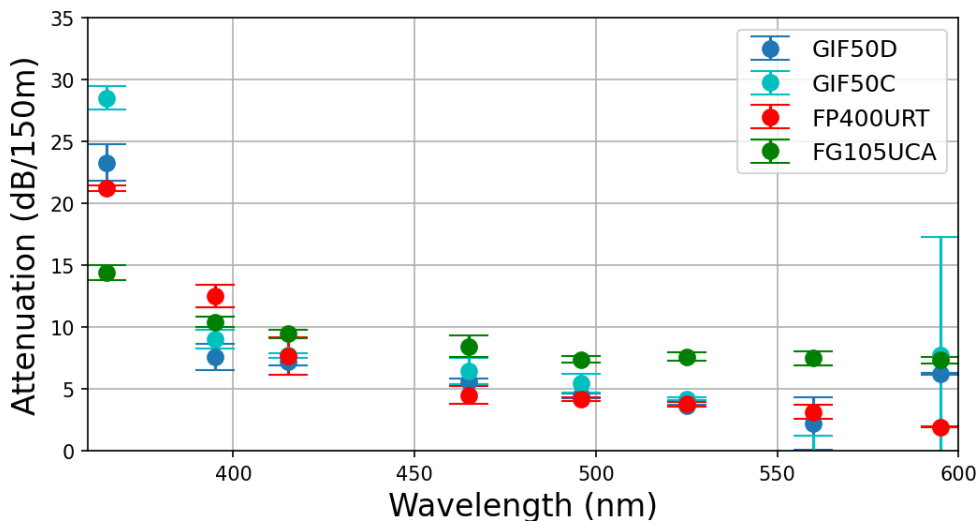


Figure 6: Measured attenuation scaled to 150 m length for all four candidate fibre types, as a function of wavelength.

277
 278 FG105UCA is the optimal fibre type to use, in terms of attenuation. Although it exhibits higher
 279 attenuation in the visible range, there is significantly less observed in the UV range, whereas the

280 other fibre options start to peak sharply in attenuation here. As lower wavelengths of light have
281 been previously observed to be more sensitive to changes in water parameters [19], prioritising
282 lower attenuation in this region should be preferred.

283 Performing these tests also provided an opportunity to become familiar with handling the fibres.
284 As was mentioned in Section 4.3.1, the long reels of fibre that were purchased for these tests were
285 done so without tubing, which is generally added in order to protect the fibres. Along with the
286 issues of light leakage previously discussed, during testing it was found that the narrow-core fibres
287 were particularly fragile, with two being broken in the process. The FP400URT fibre however
288 was seen to be far more robust and light-tight. This is attributed to its hard polymer cladding
289 and Tefzel (Teflon-based) coating, as opposed to the clear acrylate used for the graded-index and
290 FG105UCA fibres. Orders of fibre types other than FP400URT will require tubing when ordered
291 for the safety of the system.

292 **4.4 Dispersion Measurements**

293 **4.4.1 Method**

294 Similarly to the attenuation measurements described above, by the time the full lengths of fibre
295 had been ordered in, the full fibre test stand had been commissioned. Importantly, this included
296 setup of the laser system described in Section 4.1, which was used as the light source for these
297 measurements. Instead of the $\mathcal{O}(\text{ns})$ input pulse provided by the pulsed LEDs in Section 4.2.1, the
298 laser delivers a pulse of width $\sim 50 \text{ ps}$, meaning measurements would not be limited by this.

299 Various lengths of each fibre were connected in turn to the laser head, in the same way as
300 in Section 4.3.1. However, due to breakage in the attenuation testing GIF50C was not included
301 in these tests. To make timing measurements, the fibres were connected to the PMT, where the
302 signal was visualised on the oscilloscope. Across 20,000 recorded pulses, measurements were made
303 of the pulse width, negative rise time and negative fall time. Pulse widths were again defined as
304 the time above 50% of the peak voltage, while rise and fall times were defined as the time between
305 20% and 80%, or vice versa.

306 In making these measurements, another limitation of the setup became apparent; it was clear
307 from initial measurements that the measured pulse width and rise time were highly dependent on
308 the amount of light detected by the PMT. This was understood to be a limitation caused by the
309 rise time of the PMT; shorter fibres which would deliver more light due to decreased attenuation
310 exhibited longer pulse widths, as the PMT response was not quick enough. In order to get around
311 this, the measurement approach was modified. For each length of fibre tested, the laser intensity
312 was adjusted such that the output pulse would deliver approximately the same peak voltage each
313 time. This should ensure that the rise time of the PMT had no impact on the timing measurements.

314 Another issue was encountered with this setup. When making measurements with the 1 m
315 patch cable, large tails in the pulses were observed. An example of this for the FP400URT 1 m
316 cable is shown in Figure 7. Here, negative rise time and negative fall time are labelled as fall time
317 and rise time, respectively, due to the inverted nature of the pulse. It can be seen that the very
318 slowly falling tail results in a negative fall time of $6.53 \pm 0.29 \text{ ns}$, despite a negative rise time of only
319 $0.74 \pm 0.02 \text{ ns}$. This results in a measured pulse width longer than those observed for longer fibre
320 lengths, making dispersion incalculable. As the long tails diminish with increased fibre length, it is

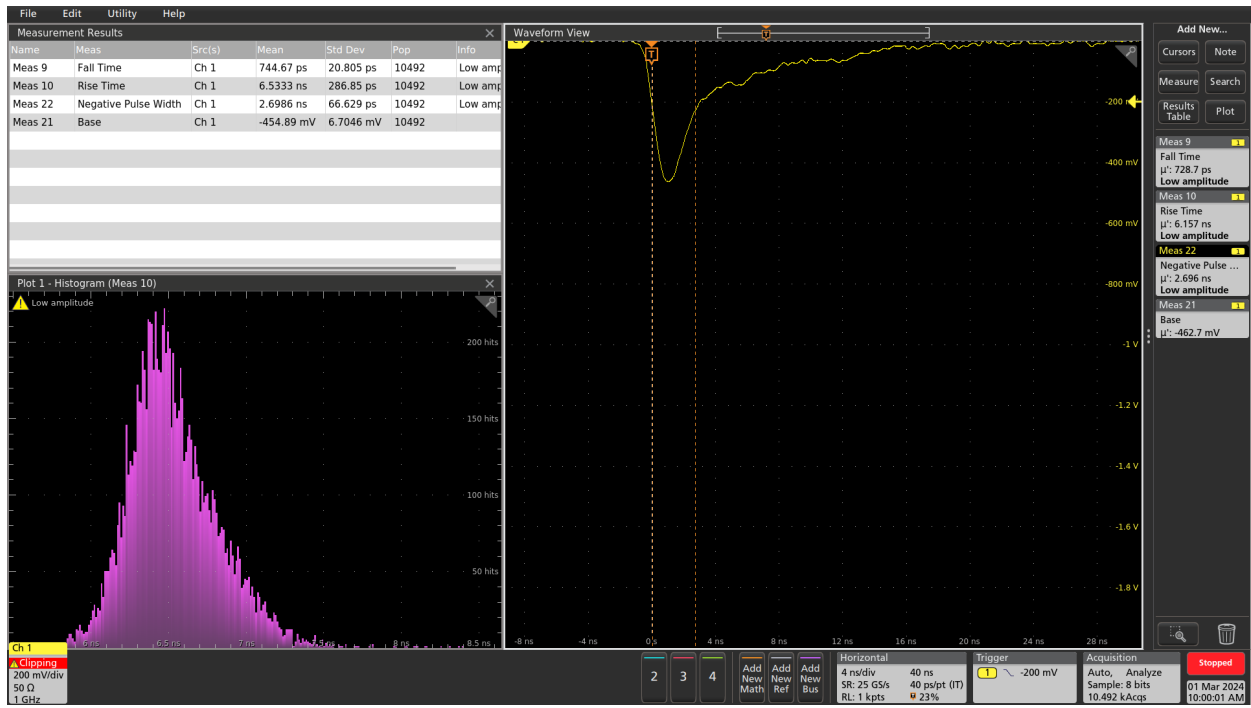


Figure 7: Scope trace and associated measurements for a 1 m FP400URT patch cable, showing the long falling tail observed.

321 thought that they are caused by reflections at the fibre coupling faces. In order to not be affected
 322 by this, measurements instead focused on the negative rise time of pulses. Unfortunately this still
 323 makes dispersion incalculable, but at least gives a way to compare pulse timing for each fibre type.

324 4.4.2 Results

325 The obtained rise time measurements for the three fibre types tested are given in Figure 8. As
 326 expected from the preliminary measurements, the fibre which exhibited the least increase in rise
 327 time was the graded-index, GIF50D, with an increase of 0.24 ± 0.03 ns. This is closely followed
 328 by FP400URT, which shows an overall increase of 0.34 ± 0.03 ns. A comparably higher increase
 329 is then observed for the FG105UCA fibre of 0.60 ± 0.05 ns. An interesting observation in these
 330 measurements is that the rise time increase is relatively sharp over the first ~ 50 m, but then
 331 plateaus toward the longest distances measured. This suggests that, should fibres be required to
 332 be longer than those tested, there should not be a substantial increase in rise time over what has
 333 already been observed. It should also be noted that, at the maximum distance of ~ 140 m, the
 334 measured rise times for all fibres are smaller than the typical 50 cm PMT rise time of 5 ns [17].

335 While these measurements give a good estimate of how timing will increase over large lengths
 336 for each fibre type, it will be important to confirm exact dispersion measurements for the chosen
 337 fibre type. As such, a high frequency readout system is currently in development, so that these
 338 measurements can be made at a later time.

339 4.5 Fibre Choice

340 Unfortunately, the results from both the attenuation and dispersion tests are diametrically opposed;
 341 while the graded index fibres performed best in terms of dispersion and pulse rise time increase,

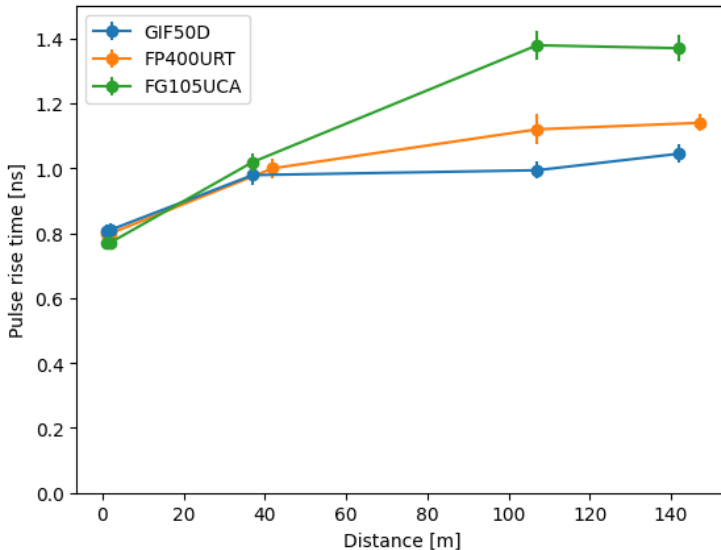


Figure 8: Pulse rise time measurements for three candidate fibres, across a range of lengths.

they exhibited the greatest amount of attenuation. The opposite is true for the FG105UCA fibre, with FP400URT performance in the middle for both tests, meaning there is not a single fibre type that is clearly preferred. Specific aspects and requirements of the two separate LI systems should be taken into account to make this choice.

Firstly, it is important to remember that the decibel scale is logarithmic, meaning that the ~ 10 dB difference between the FG105UCA and FP400URT/GIF50D fibres observed at 365 nm represents an additional $\mathcal{O}(10)$ times power loss. Therefore, the differences observed in attenuation are much greater than for the pulse width measurement, and as such the former should be prioritised as a basis for fibre decisions. While the GIF50D fibre showed the best results in terms of rise time increase, it showed significantly worse attenuation. Secondly, the ID injectors (and OD collimators) already have an internal patch fibre of FG105UCA. Coupling a wide-core fibre such as FP400URT into this narrow-core fibre will result in significant light loss at the connection point, and so should be avoided. Therefore, on balance, the FG105UCA narrow-core step-index fibre is judged to be the optimal choice for the laser system. However, the initial results for the 1 m patch cables given in Table III make it clear that coupling an LED to such a small core diameter fibre is difficult. As such, the choice for the OD LED system is the FP400URT fibre, which has a four times wider core and the next best attenuation results.

5 Fibre Switching Device

5.1 Overview

As was mentioned in Section 2, the ID laser system will require dedicated fibre switching devices in order to couple all lasers to all possible channels. To that end, two potential companies that manufacture fibre switching devices were identified, and test devices in a 1x4 configuration were purchased for evaluation. From the first company, Agiltron [20], a single 1x4 device was purchased with FP400URT as the internal fibre. A second company, Weinert Industries [21] supplied two 1x4

366 devices; one of these contained FP400URT fibre, while the other used GIF50C. All three devices
 367 are controlled via USB. It should be noted that only two companies could be found that could
 368 supply these kinds of specialist devices.

369 5.2 General Comparisons

370 To understand the performance of the three test switches, power measurements were made com-
 371 paring the output power from each of the four ports to a reference fibre of the same type. For the
 372 reference fibre measurements, two 1 m patch cables were coupled together to make a 2 m cable,
 373 with the total cable length of each of the switches being around this length.

374 Measurements were made using the 371 nm laser as the light source. The power meter was used
 375 to make measurements across 20,000 readings, where each of the four fibre outputs on a switch
 376 were selected and coupled to in turn. Power readings and calculated transmission percentages
 for the Agiltron FP400URT switch are given in Table IV. The results obtained show generally

	Agiltron FP400URT		Weinert FP400URT		Weinert GIF50C	
	Power (μW)	% of ref.	Power (μW)	% of ref.	Power (μW)	% of ref.
Reference	9.58 ± 0.01	100	9.67 ± 0.01	100	9.69 ± 0.01	100
Port 1	8.93 ± 0.01	93.11 ± 0.14	7.41 ± 0.01	76.64 ± 0.13	9.49 ± 0.01	98.09 ± 0.20
Port 2	8.67 ± 0.01	90.55 ± 0.14	7.41 ± 0.01	76.64 ± 0.13	9.59 ± 0.01	98.83 ± 0.20
Port 3	8.71 ± 0.01	91.06 ± 0.14	7.27 ± 0.01	75.18 ± 0.13	9.36 ± 0.01	96.70 ± 0.20
Port 4	8.66 ± 0.01	90.50 ± 0.14	7.00 ± 0.01	72.39 ± 0.13	9.23 ± 0.01	95.30 ± 0.20

Table IV: Power transmission across the 1x4 switching devices, with comparison to a reference cable of the same type as the device internal fibre.

377 good power transmission for all three devices tested, albeit with clearly better transmission for
 378 the Agiltron FP400URT and Weinert GIF50C than for the Weinert FP400URT. This may be in
 379 part due to the fact the fibre on the Weinert FP400URT is longer than the others (and the 2 m
 380 reference), measuring approximately 2.3 m in total. It should be noted here that, at least for the
 381 Weinert switches, any switch with more than four outputs is formed by daisy-chaining together
 382 1x4 switches. For example, a 1x16 switch would be constructed by connecting the four output
 383 channels of a single 1x4 switch into the inputs of four additional 1x4 switches. Therefore for the
 384 required 1x6 and 1x80 switches, these losses will be experienced up to six times in total. It is
 385 unclear whether the Agiltron switch is constructed in the same manner.

387 The variation in output power between ports is also generally low across the devices, with a
 388 difference of 2.61% for the Agiltron FP400URT, 4.25% for the the Weinert FP400URT and 3.53%
 389 for the Weinert GIF50C. These results suggest that the Agiltron device minorly outperforms the
 390 Weinert devices in terms of power variation across ports, whilst the Weinert GIF50C was best for
 391 transmission.

392 During ordering, setup and testing of these devices, we experienced very different degrees of
 393 assistance from the two companies. While this is not a quantifiable metric, it is none the less very
 394 important to keep in mind when making a decision for the full fibre system. The Agiltron switch
 395 arrived with no documentation on how to set up and run the device. The correct way of doing this
 396 was eventually understood out after several emails to the supplier. The Weinert switches on the

397 other hand arrived with full documentation, along with a simple software package for operation.
398 All email communication with them throughout the ordering and testing process has been very
399 helpful, if somewhat slow at times.

400 The LI system is a critical component of the HK calibration programme, and will need to
401 run for many years. It is crucial that support is available from the manufacturer of significant
402 components such as the fibre optic switch, should anything go wrong during its lifetime. The
403 experience of working with Weinert was significantly better, and this should be kept in mind when
404 selecting which device to proceed with. In particular, should issues arise with hardware in the
405 future, it would be significantly easier to deal directly with the manufacturer, rather than going
406 through a third-party distributor as with Agiltron.

407 5.3 Cross-talk Measurements

408 While making the transmittance measurements shown in Table IV for the Agiltron device, it was
409 noted that small non-zero readings were being made by the power meter whilst connected to ports
410 that were not currently being illuminated. These persisted after turning off the laser and re-zeroing
411 the power meter, and suggested some crosstalk between fibres. This is of course something that
412 should be avoided, as only one injector should be illuminated within the tank at a time.

413 In order to confirm this was the case and measure the level of crosstalk for these devices, four
414 power meters were set up, with one connected to each of the four ports on a switch, and all re-
415 zeroed at the same time. A simple python script was used to loop through the four ports 1000
416 times, before stopping at each port in turn and taking readings for ~ 10 s. This was repeated for
417 runs of approximately 18 hours per fibre switching device. Data was analysed by stripping out
418 data points from the rapidly varying periods, as well as the first and last point of each sustained
419 period where the device may still have been switching and thus not illuminating the port for the
420 entire time taken for one reading.

421 Data from this test is shown in Figures 9, 10 and 11 for the Agiltron FP400URT, Weinert
422 FP400URT and Weinert GIF50C switches, respectively. Each of these shows data taken by the
423 power meters when the port was a) illuminated and b) not illuminated. These plots show a
424 subset of the full data-taking runs in order to better show the observed structure. Figures 9a, 10a
425 and 11a, which show the readings from illuminated ports, show a similar level of variation to the
426 data presented in Table IV. The most interesting result is seen in Figure 9b, which shows clear
427 changes in the power readings recorded on ports 1 and 2, when these ports are not illuminated.
428 There is also a repeating structure to the data from port 4 suggesting a lower level of crosstalk
429 to that channel. This suggests varying levels of crosstalk between different ports. Figures 10b
430 and 11b on the other hand show no measurable cross talk between any of the channels.

431 To further investigate this, the way the data is plotted was inverted. The four plots in Figure 12
432 show the power recorded on a specific port, each separated by which of the other three ports was
433 illuminated at the time. While the absolute value of the power is not expected to be exactly zero
434 due to global drift caused by temperature changes in the lab over the course of data taking, all four
435 power meters were calibrated at the same time, so should show the same level of power when not
436 illuminated. This is clearly not the case for ports 1 and 2 (Figures 12a and 12b), with the former
437 showing higher power readings when port 2 or port 3 were illuminated, and the latter showing the
438 same when port 3 or port 4 were illuminated. There is also a small offset observed for port 4 in

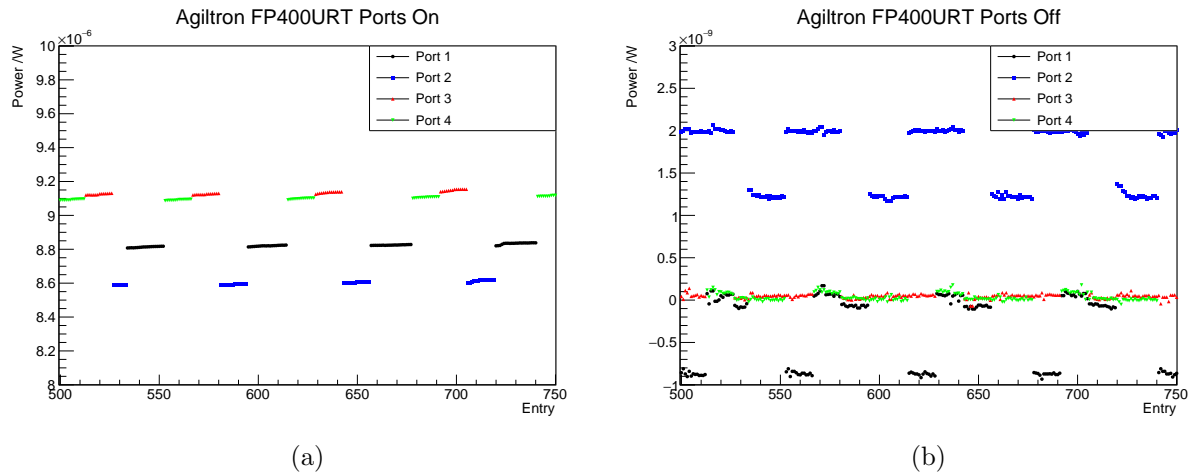


Figure 9: Power meter readings from all four ports for the Agiltron FP400URT device, zoomed into a shorter period of data to better show structure. Data is shown for when ports are a) illuminated and b) not illuminated. Note the different y-axis scales.

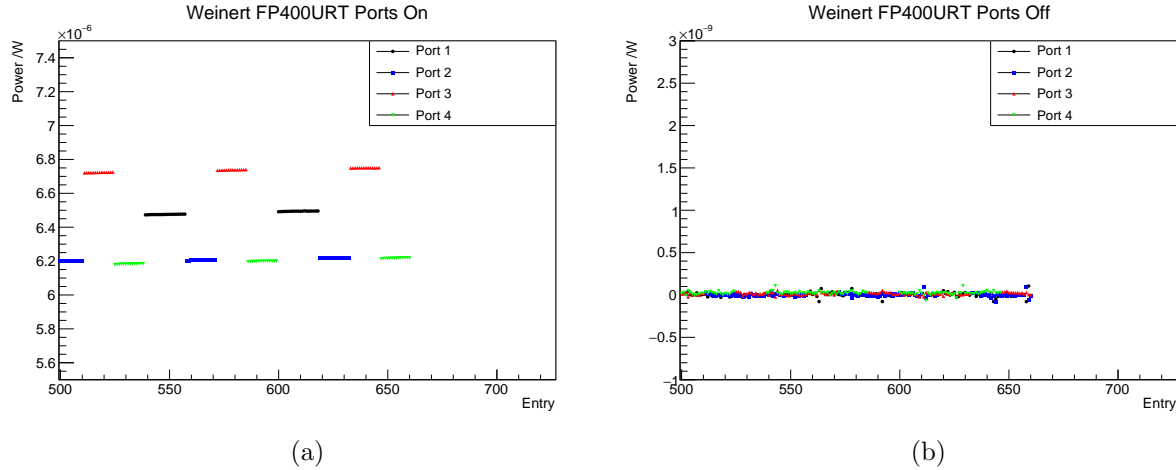


Figure 10: Power meter readings from all four ports for the Weinert FP400URT device, zoomed into a shorter period of data to better show structure. Data is shown for when ports are a) illuminated and b) not illuminated. Note the different y-axis scales.

439 Figure 12d, when port 3 is being illuminated. Interestingly, no obvious cross talk was observed to
 440 port 3, from any of the other ports being illuminated.

441 As no cross talk was observed for either of the Weinert devices, the corresponding plots are not
 442 shown here, but are given in Figures 26 and 27 in Appendix A for completeness.

443 5.4 Summary

444 Testing of the three different fibre switching devices finds different devices come out best based on
 445 different factors. The Weinert GIF50C device showed best power transmission, with at most 4.7%
 446 loss compared to the reference fibre, while the Weinert FP400URT device showed up to 27.6%
 447 loss. This is with the caveat that the device package was different, and the latter had a greater
 448 length of fibre than both the other devices and the reference fibre used. All devices exhibited under
 449 5% variation in output power across the four ports, with the Agiltron switch showing the least

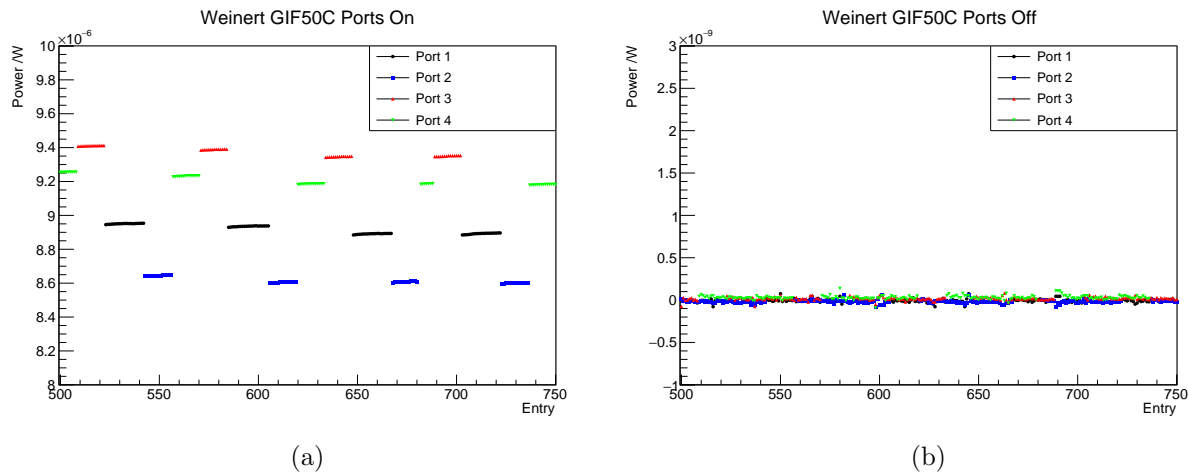


Figure 11: Power meter readings from all four ports for the Weinert GIF50C device, zoomed into a shorter period of data to better show structure. Data is shown for when ports are a) illuminated and b) not illuminated. Note the different y-axis scales.

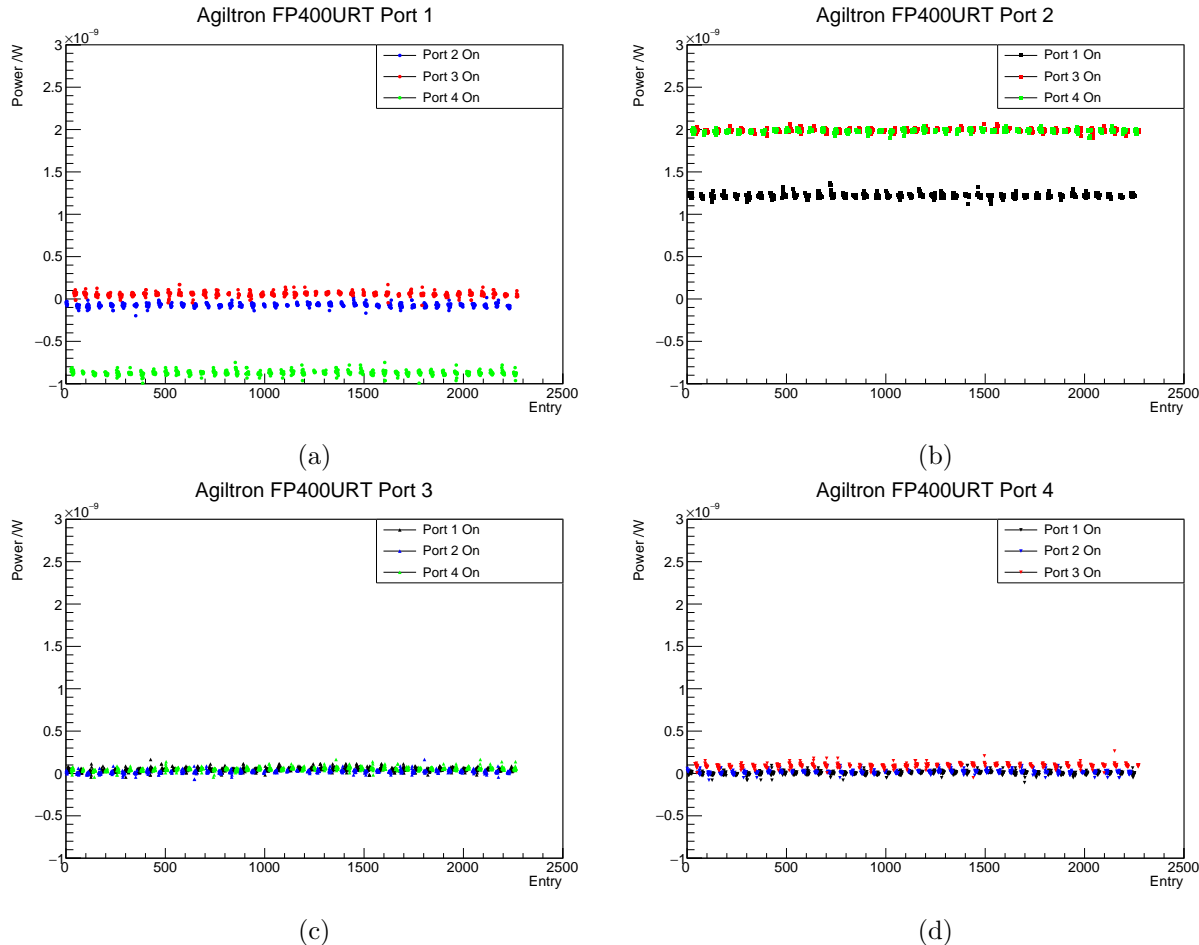


Figure 12: Power recorded on a) port 1, b) port 2, c) port 3 and d) port 4 of the Agiltron FP400URT switch, when one of the other three ports was illuminated.

450 variation at a difference of 2.61%.

451 A clear preference for the Weinert devices comes from the cross talk measurements, which show

measurable cross talk between certain channels on the Agiltron device. While this is at the level of $\mathcal{O}(0.1\%)$, the lack of any measurable cross talk from either of the Weinert devices is clearly preferable. Coupled with the superior support from Weinert which will make setup and potential servicing of the hardware easier, this is the device that is preferred. The internal fibre will of course be chosen to match what is used for the rest of the laser system, so will be Thorlabs FG105UCA or equivalent.

6 Speed of Light Measurements

As will be discussed in further detail in Section 7, the lengths of fibre optic cables connecting to the injectors will not be uniform. This presents additional challenges for the system as different path lengths result in different levels of attenuation and dispersion and, in particular, offsets in delays between signals in the electronics and actual light injection into the tank. For example, the injection event using a diffuser on the end of a ~ 160 m fibre will occur much later than when the input light has to only traverse 10 m of fibre. To account for this, delays should be incorporated into the electronics based on the expected time taken for a light pulse to be injected. To this end, the speed of light within the FG105UCA fibre was measured, to understand if this offset could be easily implemented.

Using the fibre test stand with the laser setup, the relative time delay between the laser trigger signal and the PMT signal was recorded, for fibre lengths of 1 m, 35 m, 107 m and 142 m. As with previous measurements, due to the fragility of the untubed 105 m reel of FP400URT, 1 m patch fibres were used to connect it into the system. Time delay values were recorded at each length for 20,000 events, in order to obtain uncertainties. The results for this are shown in Figure 13, where the data is fit with a linear function to calculate the necessary time delay in the electronics per metre of fibre. This verifies that the speed of light can easily be measured with this setup, and

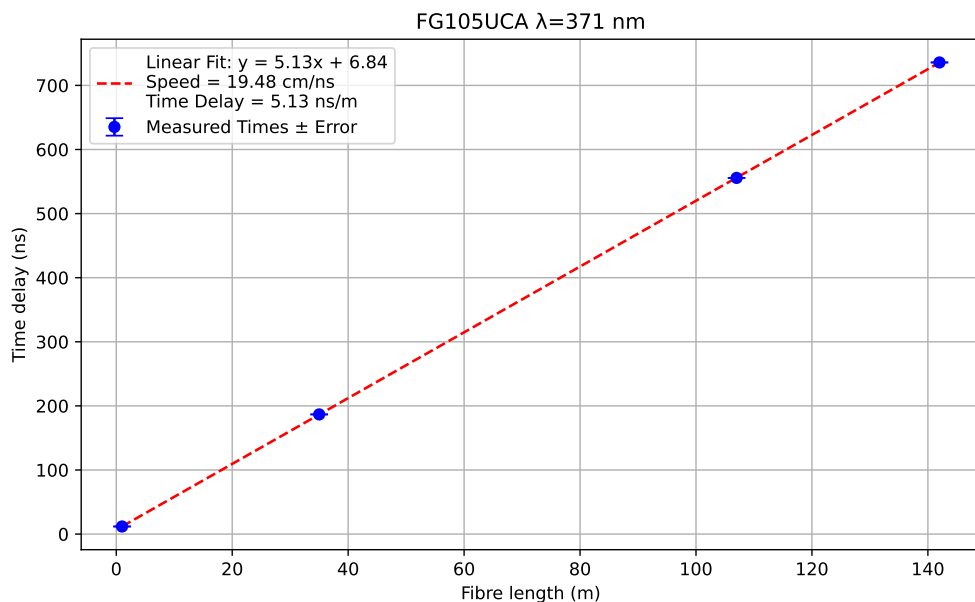


Figure 13: Time delay measurements from the FG105UCA fibres using the 371 nm laser head.

that including connectors has no obvious impact on the expected results. Naturally, as the speed

476 of light in any medium is wavelength dependent, this will need calculating for every wavelength of
 477 light used in the LI system.

478 7 Fibre Length Requirements

479 With the large number of injectors being employed for the light injection system, an even larger
 480 number of fibre optic cables will be required. This section details the quantity and lengths of cables
 481 required to connect the full HK LI system.

482 The overall design of the HK water tank and PMT support structure is given in Figure 14.
 483 Fibre optics will run through specifically installed fibre ports around the edge of the dome floor into
 the OD, then down to each injector location. 16 of these fibre ports are distributed roughly evenly

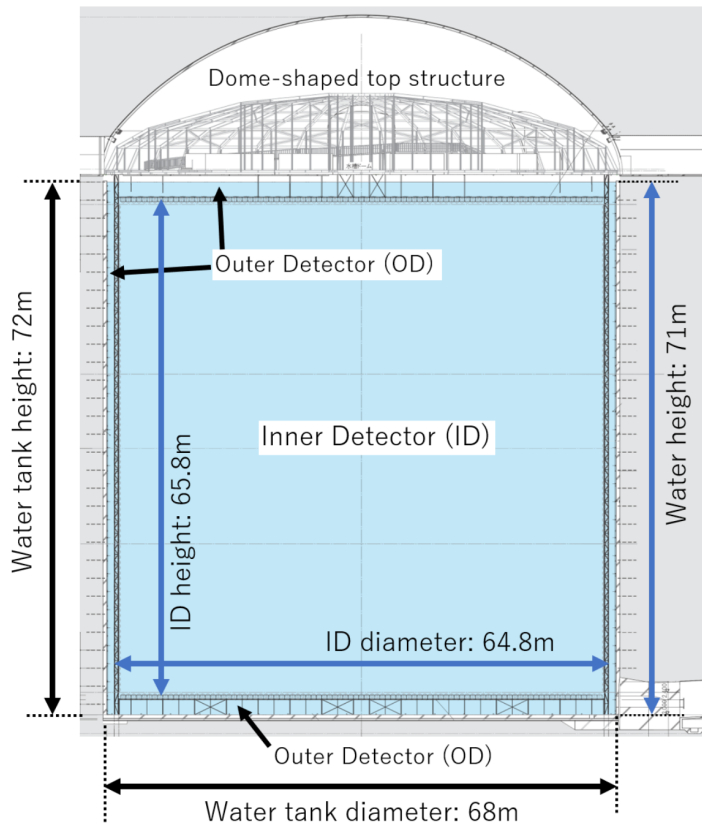


Figure 14: Schematic of the HK water tank and PMT support structure.
 [22]

484 around the outer edge of the dome. The full schematic of the dome showing all calibration and
 485 fibre ports is given in Figure 15. The OD fibre ports in question are those marked with magenta
 486 dots and labelled “odf” (OD(ニアイバー用)).
 487

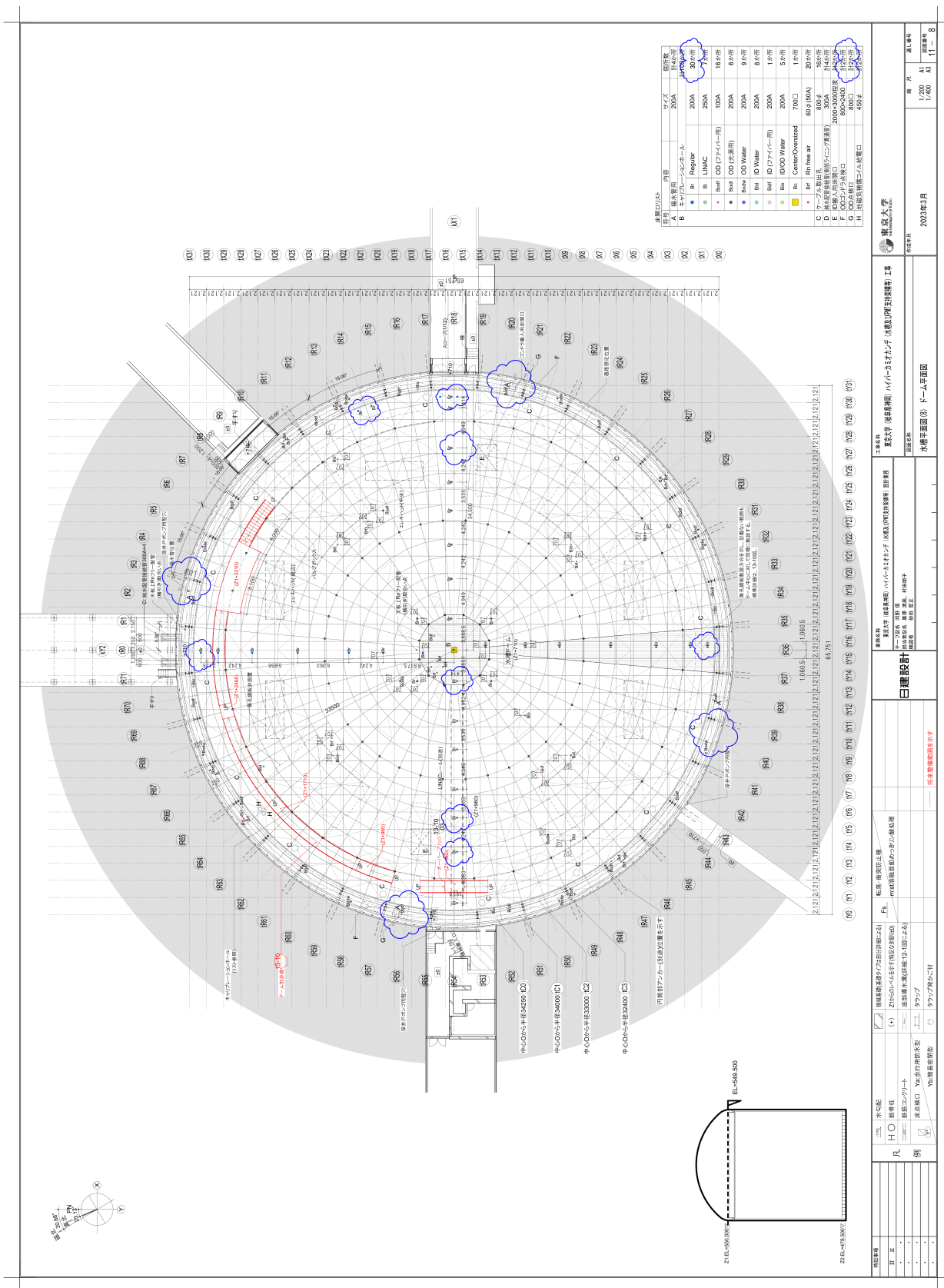


Figure 15: Top down view of the HK experimental area on top of the tank, showing locations of various calibration and fibre ports.

488 In order to limit the effect of potential damage to fibres, these will be split into in-tank and
489 out-of-tank fibres. The fibres laid along the top deck will run from the calibration rack near the
490 centre of the dome to patch panels next to the OD fibre ports. Being on the deck where there will
491 be foot traffic for up to 20 years, the out-of-tank fibres are most likely to get damaged. Keeping
492 them separate to the in-tank fibres makes replacing damaged fibres much easier, as it would be
493 implausible to replace the in-tank fibres.

494 The initial preference for the fibre layout was to keep all fibre lengths the same. While this
495 would involve many injectors being attached to fibres that were unnecessarily long, it would mean
496 that the attenuation, dispersion and timing delays of pulses sent to all injectors would be constant.
497 However, during the process of obtaining quotes, it was discovered that manufacturing a large
498 number of fibres over 100 m would be problematic for the FP400URT, as draw lengths above
499 100 m are rare. This is problematic as lengths of \sim 120 m are required to reach from the OD fibre
500 ports to the centre of the bottom end-cap. To work around this, in-tank fibres will be split into
501 two parts, one extending to the bottom of the barrel, and another extending across the bottom
502 end-cap. Connectors will be installed on the bottom corners of the tank to facilitate this.

503 With multiple in-tank fibres needing to be connected together to reach the injectors on the
504 bottom end-cap, it no longer makes sense to make all injector path lengths the same. Therefore,
505 the required lengths need to be calculated for each section, based on deployment method and path
506 taken.

507 7.1 Injector Cell Locations

508 7.1.1 Barrel Injectors

509 As shown in Figure 1, the ideal ID injector layout features seven injector layers in the ID, equally
510 separated. In reality, injector locations will be constrained by the available cells not already
511 occupied by the PMTs, cable drums or various kinds of electronics vessels within the PMT support
512 structure. Figure 16 shows an example of this, for the bottom 12 cells of a 30° section of the
513 barrel PMT support structure. There will be a total of 92 cells in the vertical direction. During
514 construction, the barrel PMT support frame will be constructed in layers of four cells at a time.
515 Once the full layer is complete and the respective components installed, the layer will be raised, and
516 the next four cells constructed underneath. During construction of each four-cell layer, scaffolding
517 will be required to work on the top two cells. To avoid this, installing injectors in the bottom
518 two cells of each four-cell layer is planned. As the bottom cell of each layer is often dominated
519 by electronics vessels, the second cell is preferable for injector locations. Dividing the total height
520 into eight parts and taking the closest second layer yields the vertical cells given in Table V. This
521 results in a set of seven vertical cells symmetrical around cell 46, the top of which is at the centre
522 of the tank. Table V also lists the z position of the bottom of the cell, using cell heights of 707 mm
523 and again treating the top of cell 46 as $z = 0$ mm. To get the injector z coordinates an offset
524 is added to each, accounting for the 125 mm width of the horizontal bars, and then assuming an
525 extra 50 mm to account for diffuser mounting and radius.

526 To define the horizontal location of cells, the radial labelling of the vertical support struts
527 shown in Figure 15 is used, starting from tR0 and running to tR71 in the clockwise direction.
528 Between each of these supports is a 5° angle, containing four cells. As no standard cell labelling

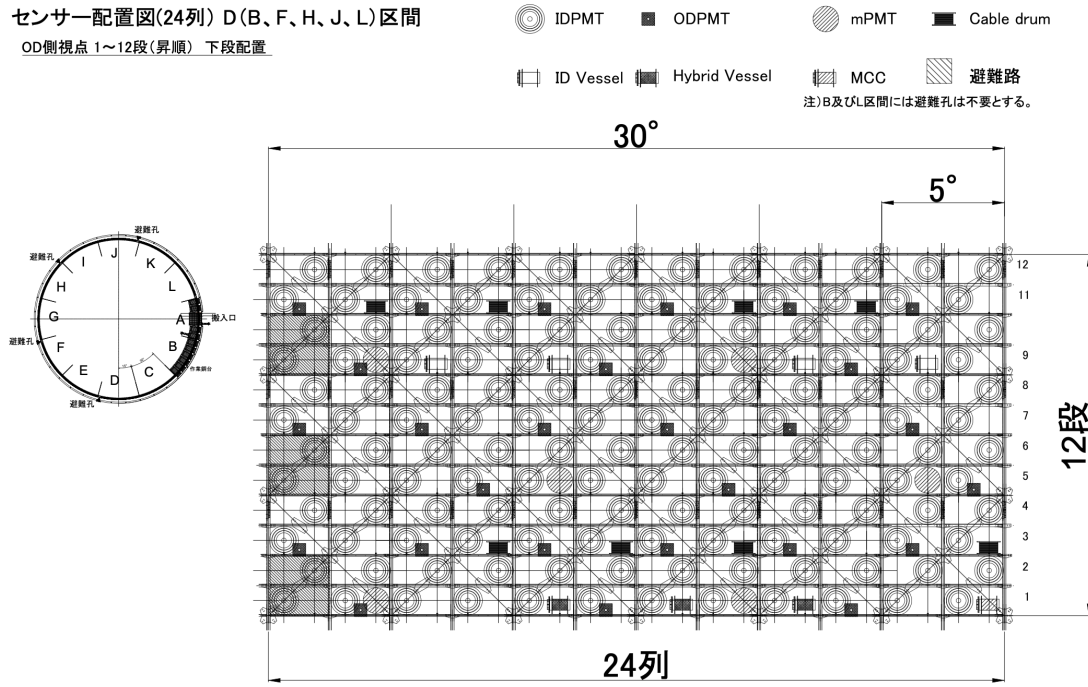


Figure 16: Diagram showing cells 1-12 of a 30° section of the barrel PMT support structure, with fixed locations of components marked, as seen from the OD side of the structure.

ID vertical label	Vertical cell	Cell z position (mm)	Injector z position (mm)
1	82	24745	24857.5
2	70	16261	16373.5
3	58	7777	7889.5
4	46	-707	-594.5
5	34	-9191	-9078.5
6	22	-17675	-17562.5
7	10	-26159	-26056.5

Table V: Vertical cell locations for both ID and OD barrel injectors. Cell z position is defined as the bottom of the cell, and injector position assumes the injector being installed at the bottom of the cell, accounting for the width of horizontal bars and radius of injectors.

529 currently exists in the horizontal, we label each cell 1 through 4, again in the clockwise direction,
 530 resulting in a horizontal cell label of the form $tR X.Y$, where $X \in \{0..71\}$ and $Y \in \{1..4\}$. As
 531 Figure 16 is viewed from the OD side, vertical support labels and cell numbers increase from right
 532 to left. **These cell addresses will be updated once a common system is decided within**
 533 **the integration group.**

534 As one column of ID injectors will coincide with the position of the Korean LI system, the
 535 horizontal positions are dictated by this. The Korean LI system will be installed between the two
 536 regular calibration ports (labelled ‘Br’ in Figure 16) either side of tR14. Based on the previous
 537 requirements for cell choice, tR13.4 is the optimal choice for injector placement in this region, for
 538 the Korean LI and the ID LI optics. Placing LI ID injectors at every 90° this sets the remaining
 539 horizontal cell locations as tR31.4, tR49.4 and tR67.4.

The OD diffuser ideal positions are shown in Figure 2, where again there are seven vertical positions within the barrel. To simplify installation, the vertical positions for the ID and OD diffusers in the barrel will be aligned. As each layer of OD barrel diffusers is offset from the previous by 15° , this results in OD diffusers in the same cells as ID injectors for only layers 1, 3, 5 and 7. Starting from the overlap cells, and placing 12 diffusers in each layer (one every 30°), results in the OD diffuser barrel cell locations listed in Table VI.

Vertical label	1, 3, 5, 7	2, 4, 6
Horizontal cell	tR1.4	tR4.4
	tR7.4	tR10.4
	tR13.4	tR16.4
	tR19.4	tR22.4
	tR25.4	tR28.4
	tR31.4	tR34.4
	tR37.4	tR40.4
	tR43.4	tR46.4
	tR49.4	tR52.4
	tR55.4	tR58.4
	tR61.4	tR64.4
	tR67.4	tR70.4

Table VI: Cell locations for OD barrel diffusers.

While the exact positions of the 12 OD collimators are yet to be set, the rough locations for mounting have been decided. Three will be installed on the edge of the top end-cap, while the other nine will be installed on the edge of the bottom end-cap.

7.1.2 End-cap Injectors

For the ID injectors, the top-end cap will have a single location. The diffuser and collimator will be installed through the ID fibre port, labelled ‘Bidf’ in Figure 15. Only one position here is needed, as the injectors can easily be removed in the case of any faults. For the bottom end-cap this is of course not possible, and so four sets of injectors will be installed around the centre for degeneracy. A diagram of an end-cap is shown in Figure 17. The locations of PMTs and electronics vessels shown will be the same for both top and bottom. Only the ports (shown in yellow) are unique to the top end-cap.

For the OD, 19 diffusers will be installed on each end-cap. The locations of these, which are again same for top and bottom, are shown in Figure 17, denoted by cyan stars. These positions are chosen to match as closely as possible to the ‘ideal’ layout shown in Figure 2. **Exact cell locations will be provided once a cell address scheme is decided upon by integration group.**

7.2 Fibre Paths

With the locations of the injectors decided, the routes of fibre optic cables to said injectors can be planned, and the required lengths of each set of fibres obtained. Installation of the majority of fibres will take place after construction of the PMT support structure is completed. A small

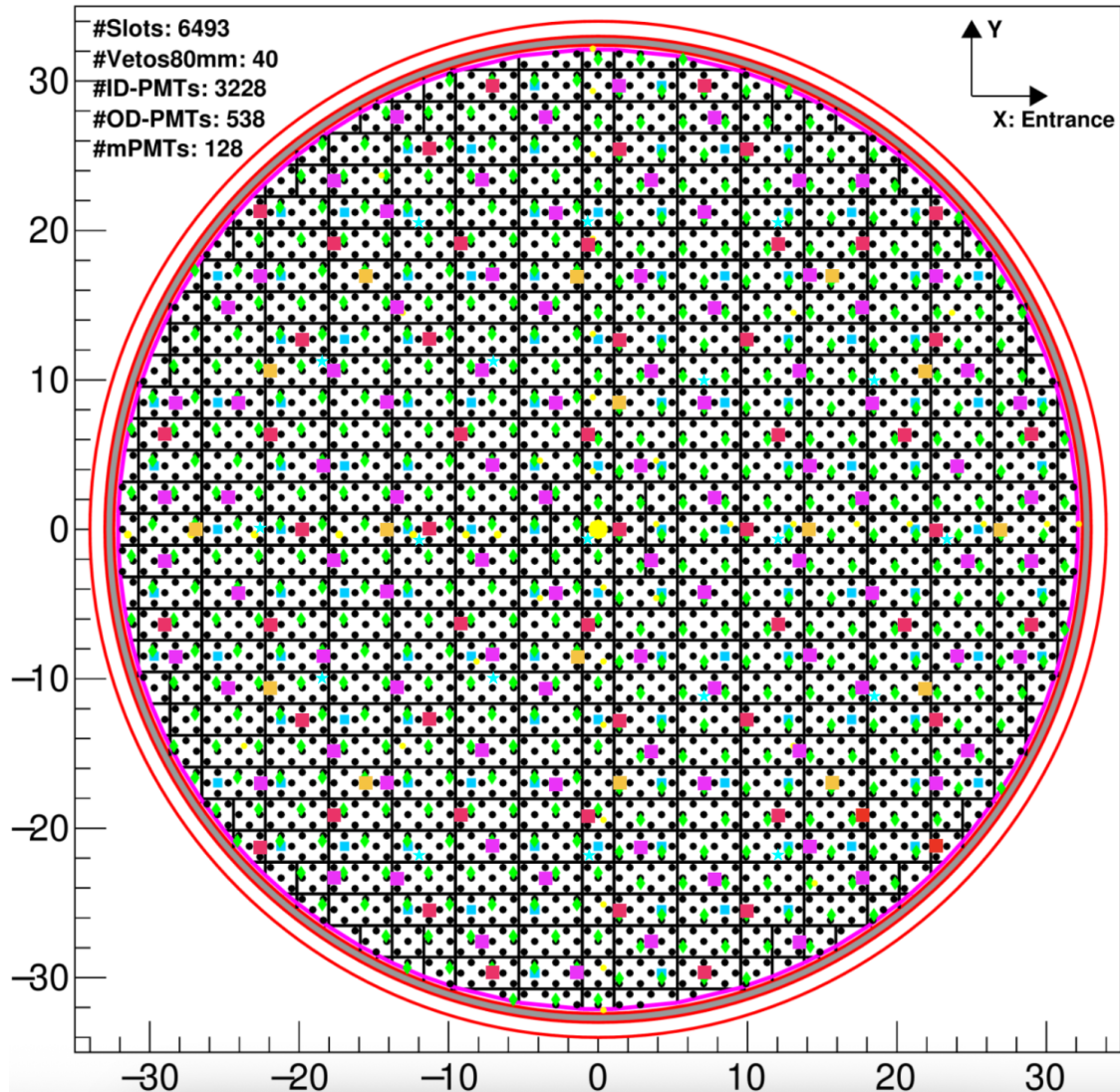


Figure 17: Diagram of PMT support structure end-cap, with a variety of components' locations shown. Other than calibration ports (yellow circles), mapping is the same for both top and bottom end-caps. The location of OD diffusers is shown with cyan stars.

team of experts will enter the tank in the OD gondola, using this to route fibres around the tank. Given the size of the Hyper-K tank, and the low speed of a gondola (initial designs estimate this at 0.2 ms^{-1}), many decisions made here are in an effort to make installation as efficient as possible.

7.2.1 Top Deck

This set of fibres is used to run from the calibration racks near the centre of the top deck, to respective OD calibration ports around the edge, where they will attach to patch panels. This will be done for all injectors except for the top ID injectors, and top OD diffusers. The preferred method for installation is for the fibres to be laid into cable trays underneath the deck, to limit the chance of breakage from exposure to foot traffic. In mapping these routes out it is assumed that the fibre can travel in a straight line from rack to port, with the exception of having to avoid any structures that penetrate the deck to the tank, such as ports and gondola hatches. The proposed routing is shown in Figure 18, though the exact location within the calibration area marked in blue

578 that the fibres would meet is as yet unknown. The only fibres which cannot travel in a straight
 579 line are those to ODF5 and ODF13, as they have to bend around the marked ID gondola hatches.
 580 Using this as a guide, the required fibre lengths can be calculated. As the point that the fibres
 581 will exit at the calibration rack is unknown, the unit 2121×2121 mm square is highlighted, and
 582 the distance to the closest edge of this measured. To account for the unknown distance within
 583 the square, and any vertical travel required up the calibration rack, an addition of 5 m will then
 be applied to every required length. The actual measurement of each fibre is done by the pixel

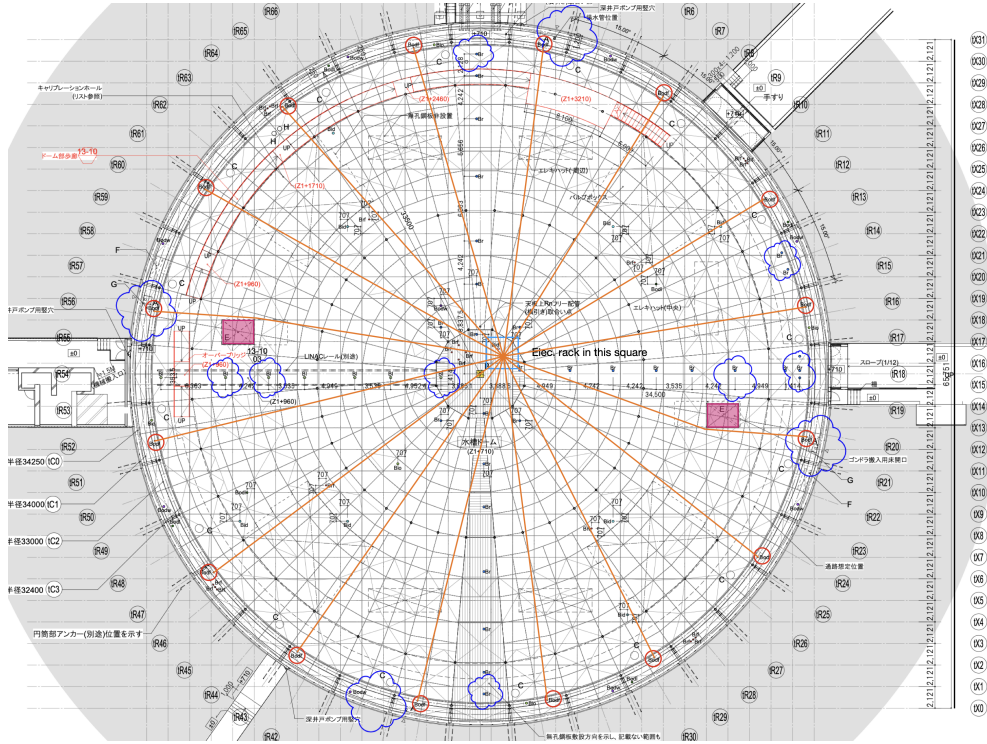


Figure 18: Diagram of fibre routing below deck from calibration rack to OD fibre ports. OD ports are circled in red, ID gondola hatches outlined in purple, and the blue square shows a $\sim 3 \times 3$ m square where the calibration racks will be. Orange lines show the proposed fibre routes.

584
 585 length of each line from rack to port. The total diameter of the tank is measured to be 984 pt. As
 586 this is shown in Figure 19 to be 65751 mm, this equates to $1 \text{ pt} = 66.82 \text{ mm} \simeq 67 \text{ mm}$. Using this,
 587 the required length of each fibre can be calculated. These values are summarised in Table VII.

588
 589 The maximum length requirement found here is 34572 mm, to get to ODF 11. Adding the 5 m to
 590 account for reaching the calibration rack and travelling vertically to the specific crate gives a total
 591 distance of 39572 mm. This can then be rounded to 42 m for safety, and to ensure the fibres have
 592 some slack in them. As both ends of the fibres will connect to patch panels, each end of the fibre
 593 should have an FC/PC connector, for both fibre types.

594 7.2.2 Barrel Fibres

595 There are two sets of fibres which need to run down the side of the barrel: those that connect
 596 to barrel injectors, and those that must run to the bottom of the tank to reach bottom end-cap

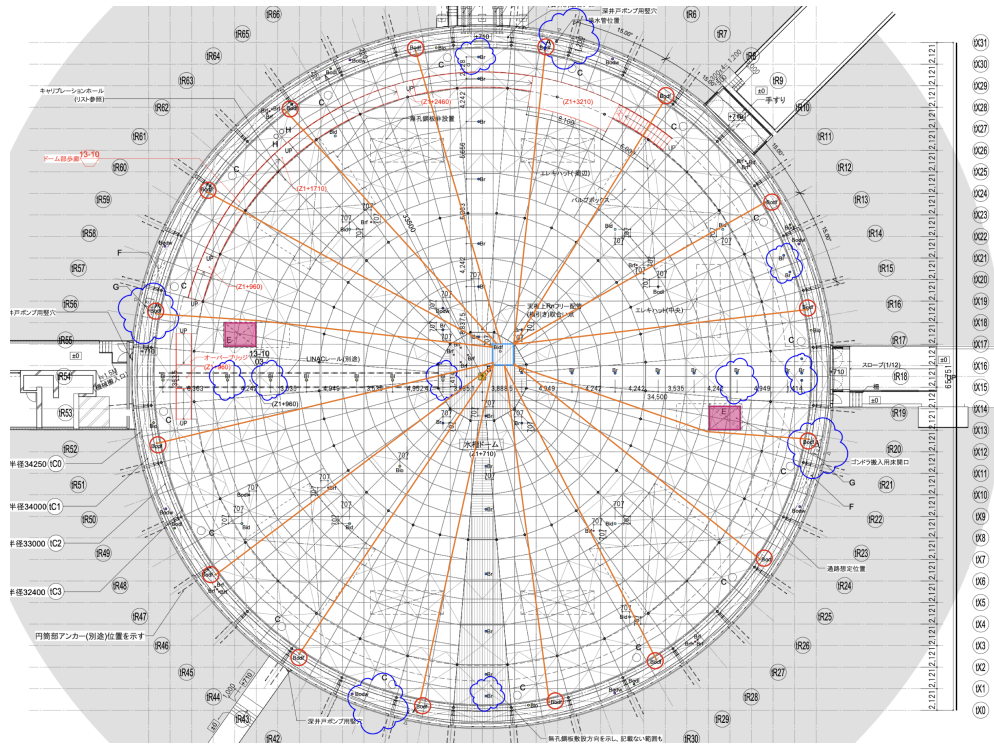


Figure 19: Same as Figure 18, except the blue square outlines the $\sim 2 \times 2$ m square within which the fibres could potentially exit the deck, as the exact location of the calibration rack is not known. In this case the orange lines are used to measure distance from respective calibration port to the edge blue square. This is not the map used for fibre routing itself.

597 injectors. As these will both take the same paths down the vertical supports, they are included
598 together here.

599 To route these fibres to either a barrel injector or bottom end-cap, the fibres will run through
600 one of the 16 OD calibration ports. These ports extend 1200 mm below the top of the tank, into the
601 dead region of the PMT support structure. At the point where the fibres exit the port, they will be
602 routed to one of the two neighbouring vertical supports. The support chosen will not necessarily
603 be the closest one, as choices should be optimised for efficient installation. The mapping between
604 horizontal cell location, fibre port, and vertical support to route down is shown in the first three
605 columns of Table VIII. As should be clear from this, the majority of injectors will not have the
606 fibre run directly down to them. Instead, each fibre will run down the respective vertical support
607 until at the same horizontal level as the injector, before being running radially around the side of
608 the detector to reach the injector cell. In both ID and OD cases this will be done on the outer edge
609 of the support structure; for OD diffusers this is where they will be housed. For the ID injectors,
610 a patch cable to span the dead region will have been installed at the same time as the injector
611 housing itself, to avoid the person connecting the fibre having to reach out of the gondola into the
612 dead region.

613 To calculate the maximum amount of additional fibre needed to account for this horizontal
614 travel, the angular difference between each injector cell and the respective vertical support used to
615 route down can be calculated. This is done assuming the injector is installed in the centre of a cell,
616 with the values given in the final column of Table VIII. Taking the maximum angular difference of

Port ODF no.	Length [pt]	Length [mm]	Port ODF no.	Length [pt]	Length [mm]
1	437	29279	9	512	34304
2	426	28542	10	515	34505
3	427	28609	11	516	34572
4	437	29279	12	513	34371
5	$152 + 301 = 453$	30351	13	$153 + 349 = 502$	33634
6	465	31155	14	481	32227
7	489	32763	15	468	31356
8	503	33701	16	451	30217

Table VII: Required length of fibre to reach from each OD fibre port to the 2121×2121 mm square the calibration rack is assumed to be in.

617 10.625°, an arc length of 6130 mm is found. The same has to be done for the distance between the
 618 OD fibre port and the vertical support. As the locations of the ports are not precisely documented,
 619 the maximum angular distance of 5° is taken, equating to 2885 mm. These additions will apply
 620 to all barrel injectors. For the fibres needed to reach the bottom, only the horizontal addition for
 621 port to vertical distance is required.

622 Vertical and total length requirements for the barrel fibres are easily found from the vertical
 623 cell locations given in Table V, using a cell height of 707 mm, and a distance from the deck to top
 624 of cell 92 of 3935 mm. This again uses a bar width of 125 mm, and assumes a 50 mm offset to
 625 account for the height of the injector. The calculated values are shown Table IX. These numbers
 626 show that the additional horizontal fibre required to reach from vertical supports to an injector cell
 627 is not a problem, as the maximum length case still comes from reaching to the bottom of the barrel.
 628 For contingency, and to allow fibres to not be kept taught, the maximum length requirement is
 629 rounded up to 76 m. For the ID system, all fibres will have FC/PC connectors on either end. This
 630 is the same for the OD system fibres which traverse the entire barrel depth to the bottom end-cap.
 631 For the fibres connecting to OD barrel diffusers however, these will be polished fibre on one end,
 632 as this is what has to be pushed into the back of the diffuser hemisphere.

633 The plans presented here are used to calculate the maximum required length. Rather than have
 634 all fibres that traverse the barrel the same length, an alternative option is to split into three sets
 635 of fibres so that the amount of excess fibre can be limited, particularly for the higher up injectors.
 636 In this case, there is one length for vertical labels 1 and 2, one for 3, 4 and 5, and one for 6, 7,
 637 and fibres to the bottom of the barrel. The lengths of these are calculated using the values from
 638 Table IX, and are given in Table X. From both a cost and installation perspective, this case using
 639 three different lengths of fibre for the barrel injectors is the preferred method.

640 As mentioned in Section 7.1.1, there will also be 12 OD collimators affixed to the barrel/end-
 641 cap edges; three on the top and nine on the bottom. The bottom collimators will require the
 642 aforementioned amount of fibre needed to reach the edge of the bottom end-cap. For the top ones,
 643 which will also be connected through the OD fibre ports, a length of 10 m will be enough to connect
 644 these.

Inj. cell	ODF	Vertical to route down	Port to inj. angle [°]
tR1.4	1	2	0.625
tR4.4	2	6	5.625
tR7.4	2	6	9.375
tR10.4	3	12	5.625
tR13.4	4	15	5.625
tR16.4	4	15	9.375
tR19.4	5	20	0.625
tR22.4	6	25	10.625
tR25.4	6	25	4.375
tR28.4	7	29	0.625
tR31.4	8	33	5.625
tR34.4	8	33	9.375
tR37.4	9	38	0.625
tR40.4	10	43	10.625
tR43.4	10	43	4.375
tR46.4	11	47	0.625
tR49.4	12	52	10.625
tR52.4	12	52	4.375
tR55.4	13	57	5.625
tR58.4	13	57	9.375
tR61.4	14	61	4.375
tR64.4	15	65	0.625
tR67.4	16	70	10.625
tR70.4	16	70	4.375

Table VIII: List of all barrel injector horizontal cell locations, with corresponding OD fibre port to route through, vertical support to route down, and angle between the given vertical support and the injector cell. This assumes injector installation in centre of cell.

Vertical label	Layer	Vertical dist. from deck [mm]	Total dist. from port [mm]
1	82	11617.5	20632.5
2	70	20101.5	29116.5
3	58	28585.5	37600.5
4	46	37069.5	46084.5
5	34	45553.5	54568.5
6	22	54037.5	63052.5
7	10	62521.5	71536.5
Bottom	0	70412.5	73297.5

Table IX: Vertical and total travel distance to reach to a given layer of barrel injectors. Both distances are calculated from the deck, but the total distance takes into account maximum required travel from port to vertical and vertical to injector. Only the port to vertical distance is added for fibres extending to the bottom end-cap.

Region	Length [m]
1+2	32
3+4+5	58
6+7+bottom	76

Table X: Total length requirements for barrel fibres, in the case where lengths are split for different barrel regions to reduce excess fibre.

7.2.3 Bottom end-cap

To reach the injectors on the bottom end-cap, a final set of fibres is required. These will run from the connectors installed on the bottom edge of the PMT support structure, to a given injector position. In order to simplify installation, the bottom end-cap cable mapping is optimised to only run from four vertical supports, minimising the number of times the gondola will need to traverse the full height of the tank. In doing this ODF4 is also avoided, as this is the port that the Korean injector fibres will also run through, and it is preferable to not overload a single port or vertical support with fibres. The proposed fibre routing map for the bottom end-cap OD diffusers is shown in Figure 20. This involves having connectors at the bottom of verticals tR12, 33, 52 and 65, and thus will utilise ports ODF 3, 8, 12 and 16 for the barrel segments of these fibres, respectively. From the connector, the end-cap portion of the fibre will be routed to the ID side of the support structure, at the closest point where the orthogonal bars shown in Figure 20 meet it. The fibres must then follow this orthogonal path to reach the injectors. Required fibre lengths are measured simply by counting the unit lengths they must traverse, where the 3×3 cell size defines $1u = 2121$ mm. These lengths are given in Table XI for each OD end-cap bottom (ODEB) diffuser. As would be expected, the greatest length of fibre is needed to reach the diffuser position in the centre, ODEB10. This needs a distance of $18u = 38178$ mm. In order to simplify things, this is rounded to 42 m, matching the lengths needed for the deck fibres described in Section 7.2.1. All of these OD diffuser fibres will need to have an FC/PC connector on one end, and polished bare fibre on the other.

Not shown here are the ID injector positions. Each of the four sets will be positioned in one of the four 3×3 cell squares diagonally adjacent to the central square. The longest fibre for these is

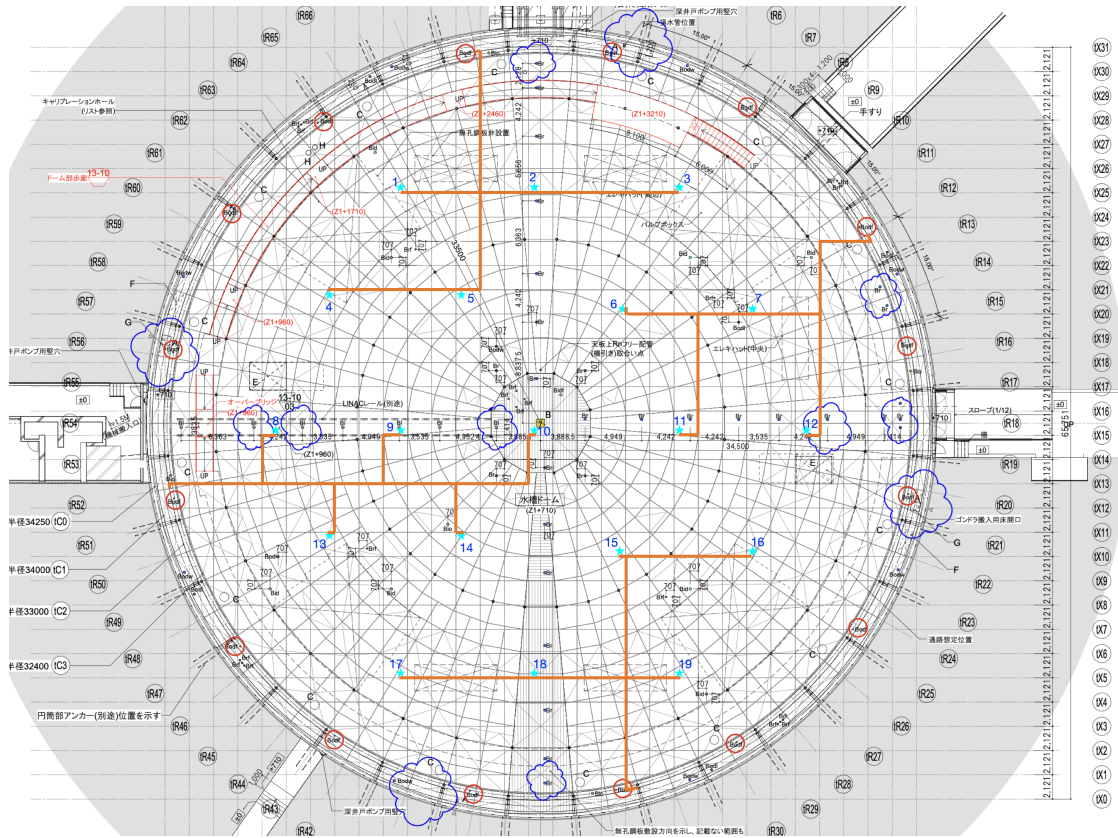


Figure 20: Map of OD diffuser positions on end-cap (cyan stars), showing fibre routing plan specifically for the bottom end-cap. Schematic shown is for the deck so port positions do not apply, but diffuser positions are the same on top and bottom.

ODEB	Vertical	Distance [u]	ODEB	Vertical	Distance [u]
1	65	10	11	12	17
2	65	9	12	12	12
3	65	15	13	52	10
4	65	17	14	52	15
5	65	11	15	33	12
6	12	15	16	33	17
7	12	9	17	33	16
8	52	8	18	33	10
9	52	13	19	33	9
10	52	18			

Table XI: Required distance of fibre optic cable to reach each OD end-cap bottom (ODEB) diffuser, in units of 2121 mm. Also shown is the vertical support that the fibre will be routed from the bottom of.

required to run from vertical tR33 to the top right injector, measuring a length of $19u = 40299$ mm. This is still below the decided 42 m length, so causes no issues. **Exact cell location will be updated once we have a decided system.** These fibres will require FC/PC connectors on both ends.

7.2.4 Top end-cap

As previously mentioned, the ID injectors for the top end-cap will be deployed through the Bidf calibration port, meaning that they can be easily removed and replaced should the need arise. In this case, only one section of fibre is needed to go from the injectors to the calibration rack. The length of these is chosen as 10 m, well above the 4506 mm height of the described port. Both ends of these fibres will require FC/PC connectors on. This also matches to the length chosen for the top OD collimators.

The OD diffusers on the top end-cap (labelled ODET 1–19) will be installed in exactly the same x and y locations as for the bottom end-cap. The difference is in the fibre routing, as there is no easy way to get the fibres from an OD fibre port back up to the top end-cap frame. Instead, all of these fibres will also be routed through the Bidf calibration port, and then spread out from this position to each respective diffuser. The fibre routing map for this is given in Figure 21. In a

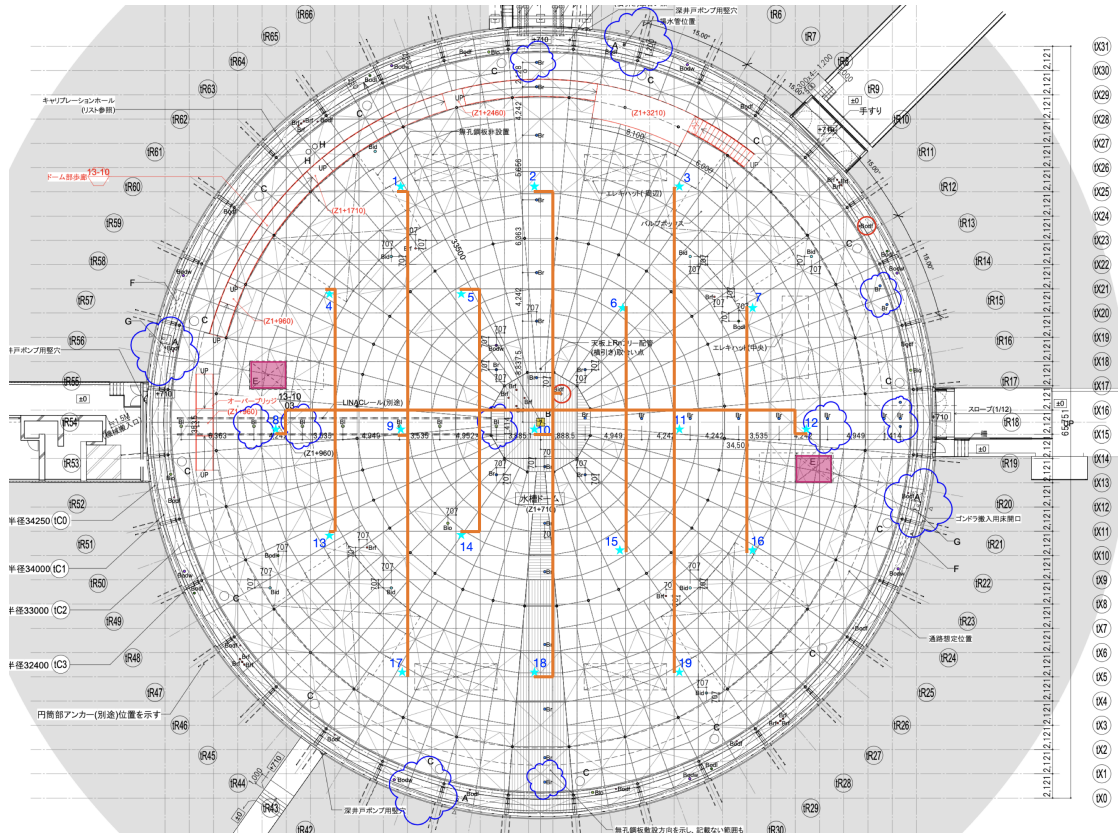


Figure 21: Map of OD diffuser positions on end-cap (cyan stars), showing fibre routing plan specifically for the top end-cap. All fibres will be deployed through the Bidf calibration port.

similar way to Section 7.2.3, the required lengths for these fibres are measured simply by counting the unit lengths along each path. The fibre lengths needed for each injector are given in Table XII. The greatest length of fibre required comes from connecting to ODET17, the furthest injector from the calibration port. This requires 19 units of length, equating to 40299 mm. Adding on 4506 mm for the height of the calibration port, and then 3000 mm for travel to the electronics rack, a maximum requirement of 47805 mm is obtained. The length of these fibres is therefore rounded to 50 m for contingency. As with the other fibres connecting directly to the OD diffusers, these will need to have FC/PC connectors on one end, and a polished bare fibre on the other. It should

ODET	Distance [u]	ODEB	Distance [u]
1	18	11	8
2	10	12	14
3	17	13	17
4	17	14	11
5	11	15	11
6	10	16	16
7	15	17	19
8	15	18	14
9	10	19	18
10	4		

Table XII: Required distance of fibre optic cable to reach each OD end-cap top (ODET) diffuser, in units of 2121 mm.

691 be noted that installation of injectors and fibres on the top end-cap is planned to be carried out by
 692 company workers rather than researchers, due to additional complications foreseen in this work.

693 7.2.5 Patch Fibres

694 Along with the long lengths of fibres described in the previous sections, a large number of patch
 695 fibres will be required at various points within laser and LED systems.

696 As described in Section 7.2.2, to connect to all ID injectors bar the top end-cap ones an ad-
 697 dditional patch fibre is also required. ID injectors will be installed on the PMT support structure
 698 during construction, while the fibre installation will be carried out after construction of the struc-
 699 ture has been completed, by utilising the OD gondola. In order to avoid workers having to reach
 700 far out of the gondola, through the support structure, to attach fibres to the injector housing,
 701 short patch fibres will be attached to the injectors at the time of their installation. These will
 702 span the dead region and be fixed to the outer side of the structure, so that the long fibres can be
 703 connected directly to the patch fibres. As part of this a fibre guide will be used, to ensure that the
 704 end of the fibre will be pointing vertically upwards for connection, without the fibre being pushed
 705 past its bending radius. The required lengths have been measured using a mockup of the support,
 706 obtaining values of 640 mm for the diffuser and 530 mm for the collimator. Both ends of these
 707 patch fibres will need to have FC/PC connectors.

708 Based on Figure 3, eight patch fibres will be required for within the laser system itself, not
 709 including the five that will come coupled to the laser heads. Five of these will run from individual
 710 attenuators to connect the laser heads to the 1x8 switch, and then three are used for the connections
 711 between the 1x8 and 1x80 switch, which includes integrating the fibre splitter for the monitor PMT.
 712 These will all be FG105UCA fibres with FC/PC connectors on either end, with a rough length
 713 requirement of \sim 50 cm.

714 A series of short patch fibres will also be required for the LED system. Each LED pulser board
 715 will feature a connector sitting atop the surface mounted LED, with space for two fibres to be
 716 inserted. One of these will be directly above the LED to collect as much light as possible, and
 717 this will be used for illuminating the OD diffusers. The second will be offset, collecting some of
 718 the remaining light to be used as a signal for monitoring purposes. As the monitor system will
 719 sit at the electronics rack, much less fibre will be used and therefore less initial light input is

720 required. The design for the the fibre connector is currently ongoing, and will be used to confirm
 721 the required length of the patch fibres within the pulser board crates. Initial measurements of the
 722 required lengths, which are different due to the topology of the connector, give 21.1 ± 1.4 cm and
 723 18.4 ± 0.6 cm, where the uncertainties here are the measured tolerances on the length. Any shorter
 724 than this and the cable will not reach. If the cables are longer, they would be required to bend at
 725 a greater angle than their specified bending radius, which will cause degradation over the lifetime
 726 of the system. As the connector for the LED pulser board will have the fibres epoxied in, each of
 727 these patch cables will require FC/PC connectors on one end, with the other cleaved and polished.

728 The final set of patch cables for the LED pulser system is that used to connect to the monitor
 729 PMTs. The internal patch cable from the LED connector will go into a patch panel on the front
 730 of the electronics rack. These patch cables will carry light from that patch panel to a system
 731 of several monitor PMTs in the same electronics rack. These will be 1 m long, with an FC/PC
 732 connector on the patch panel end, and polished bare fibre at the PMT-facing end.

733 Tables XIII and XIV summarise all the required fibres for the laser and LED systems respec-
 734 tively, detailing the chosen type, length, connectors and quantities needed. Quantities are also
 735 detailed for the cases where the fibres that traverse the barrel region are split into different lengths
 736 to minimise excess, which is the preferred approach for this system.

Length [m]	Connector A	Connector B	Required no.	Use
76	FC/PC	FC/PC	73	Barrel (all) [†]
42	FC/PC	FC/PC	84	Deck and bottom
10	FC/PC	FC/PC	5	Top ID inj. and top OD coll.
0.64	FC/PC	FC/PC	32	ID diffuser patch cable
0.56	FC/PC	FC/PC	32	ID collimator patch cable
0.5	FC/PC	FC/PC	8	Laser system patch cable

[†] Alternate staged approach:				
32	FC/PC	FC/PC	16	Barrel (levels 1+2)
58	FC/PC	FC/PC	24	Barrel (levels 3+4+5)
76	FC/PC	FC/PC	33	Barrel (levels 5+6+bottom)

Table XIII: List of all required fibres for the laser system with necessary lengths, connector configurations, quantities and uses.

Length [m]	Connector A	Connector B	Required no.	Use
76	FC/PC	FC/PC	19	Barrel to bottom
76	FC/PC	Bare	84	Barrel injs (all) [†]
50	FC/PC	Bare	19	Top diffusers
42	FC/PC	FC/PC	103	Deck
42	FC/PC	Bare	19	Bottom diffusers
1	FC/PC	Bare	122	Crate to monitor PMT(s)
0.21	FC/PC	Bare	122	Crate internal patch 1
0.18	FC/PC	Bare	122	Crate internal patch 2

†Alternate staged approach:				
32	FC/PC	Bare	24	Barrel (levels 1+2)
58	FC/PC	Bare	36	Barrel (levels 3+4+5)
76	FC/PC	Bare	24	Barrel (levels 5+6)

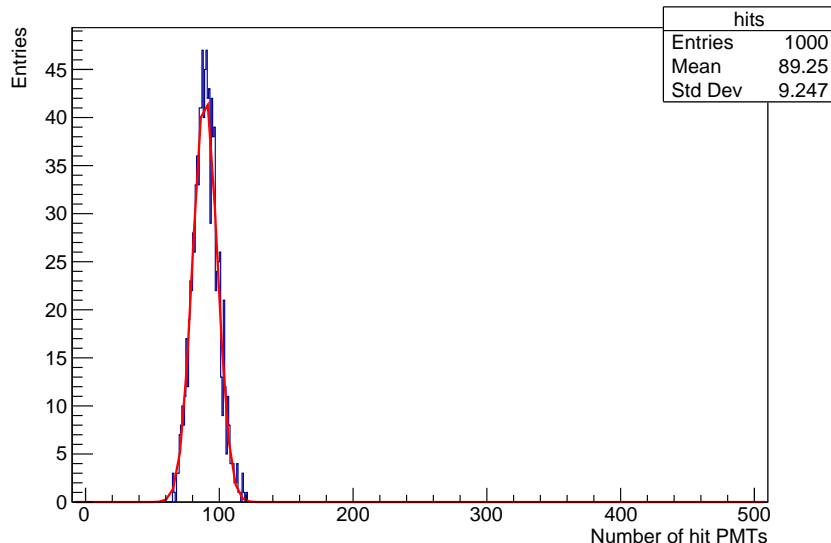
Table XIV: List of all required fibres for the LED system with necessary lengths, connector configurations, quantities and uses.

737 8 Photon Yield Requirements

738 With a series of points in the system where light can be lost, it is important to verify the number
 739 of photons required to be injected into the tank for calibration, and the initial laser power required
 740 to achieve this. This section describes the study performed to calculate these required numbers.

741 A series of simulations were run using the Monte Carlo generation package for Hyper-K, WCSim
 742 [23], using diffusers at each vertical depth level (injector indices 0, 4, 8, 12, 16, 20, 24), along with
 743 one on the top end cap (28) and one on the bottom (32). For each injector, sets of simulations were
 744 run with injected light at wavelengths of 365 nm, 395 nm, 415 nm, 465 nm, 496 nm and 525 nm.
 745 These are a subset of the wavelengths used for attenuation measurements in Section 4.3.1 and,
 746 although not necessarily the exact wavelengths that will be used in the system, allow for explicit
 747 calculation of loss factors due to attenuation without interpolating between measurements. Within
 748 each of these sets, a number of simulations were run at differing values of injected photons, initially
 749 increasing in steps of 200, before moving to larger steps for the higher wavelengths which required
 750 greater numbers. For all simulations, 1000 events are run, using nominal water parameters. The
 751 injector is treated as an ideal diffuser, with a 40° opening half-angle, and dark noise was disabled.

752 The aim for general running of the diffusers is 1% PMT coverage within the diffuser spot, and
 753 so this is used as the target for these studies. For each of the 1000 events in a simulation, the
 754 number of hit PMTs within the diffuser spot is calculated and histogrammed. This is fit with a
 755 Gaussian distribution, and the mean of that taken to be the number of hit PMTs within the spot.
 An example of this distribution is shown in Figure 22. The obtained mean can then be compared



756
 757 Figure 22: Number of hit PMTs in the spot of diffuser 0, for 1000
 758 injected photons at a wavelength of 365 nm.

759 to the total number of PMTs within the diffuser spot, to calculate the percentage coverage. This
 760 is repeated for all simulations, and compared to the 1% requirement for all injectors to obtain the
 761 minimum number of injected photons required.

762 The coverage percentages for all nine injectors for the 365 nm wavelength are given in Figure 23.
 763 The shape of these plots can be understood by thinking about the geometry of the detector.
 764 Injectors 0 and 24 are the barrel injectors closest to the bottom and top endcaps respectively, so

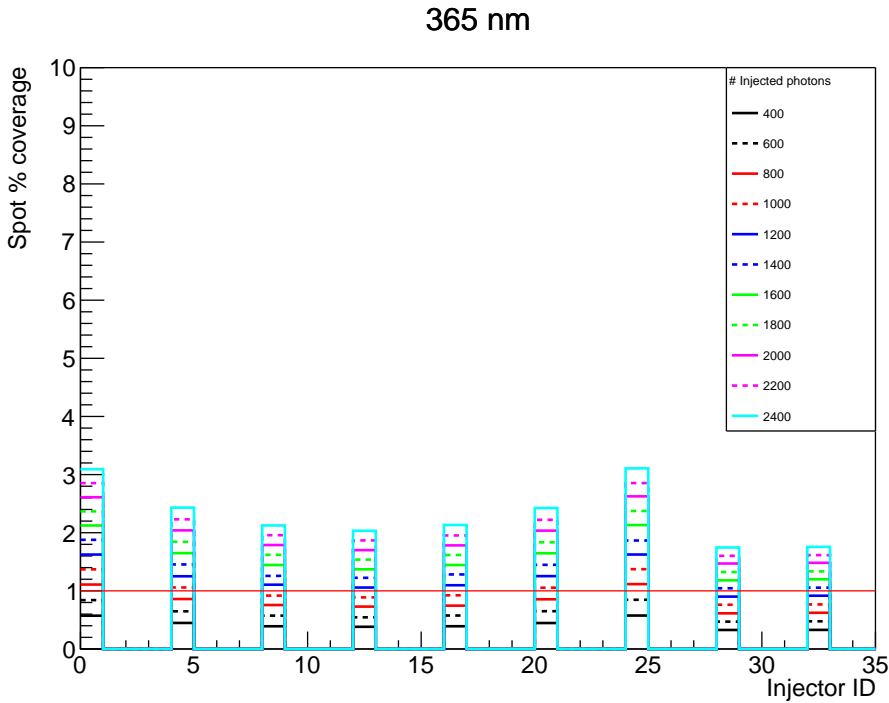


Figure 23: Coverage percentages as a function of diffuser position, for differing numbers of injected photons of 365 nm wavelength. The 1% level is shown by the red line.

those diffusers illuminate a large part of the respective end caps. The shorter path lengths between these injectors and the endcaps results in a greater amount of the initial photons causing hits, and therefore less required for 1% coverage. As the injector positions move towards the middle, there is less to no overlap with the end caps, increasing the average path length to PMTs. The final two injectors, those on the top and bottom end caps, have the greatest distance to the opposite side of the tank. There are therefore more PMTs in the spot, and with the greater distance photons are required to travel, means a greater number of injected photons are needed for 1% coverage. At this wavelength, 1400 injected photons are required to obtain at least 1% coverage in all injectors. The behaviour described repeats for all wavelengths checked, making the top and bottom injectors the limiting cases for each.

The approximate number of photons required to achieve 1% spot coverage per wavelength is given in Table XV. These numbers can then be used to calculate the required laser power per wavelength, accounting for loss due to attenuation in the fibres and other points of inefficiency within the system. The attenuation coefficients calculated in Section 4.3.1 for the above wavelengths are used to obtain the attenuation factors for the fibres, assuming the 175 m calculated in Section 7. The fibre is assumed to be the Thorlabs FG105UCA favoured in Section 4.5.

Additional light loss factors are also added into the calculations. A 90% loss is included to account for the efficiency of the ID diffuser. To account for losses in the fibre switch, we use the worst case scenario from the Weinert FP400URT measurements, and assume a 25% loss at each stage of the switch. As any larger switch is formed by daisy-chaining 1x4 switches, this 25% loss can be experienced up to 6 times (twice for a 1x8 switch plus four times for a 1x80 switch), resulting in an efficiency of $0.75^6 \simeq 0.18$. As the Weinert GIF50C results showed much greater transmission

Wavelength (nm)	N photons for 1% coverage
365	1400
395	1200
415	2000
465	3000
496	6000
525	24000

Table XV: Approximate number of injected photons required for 1% diffuser spot coverage, per wavelength.

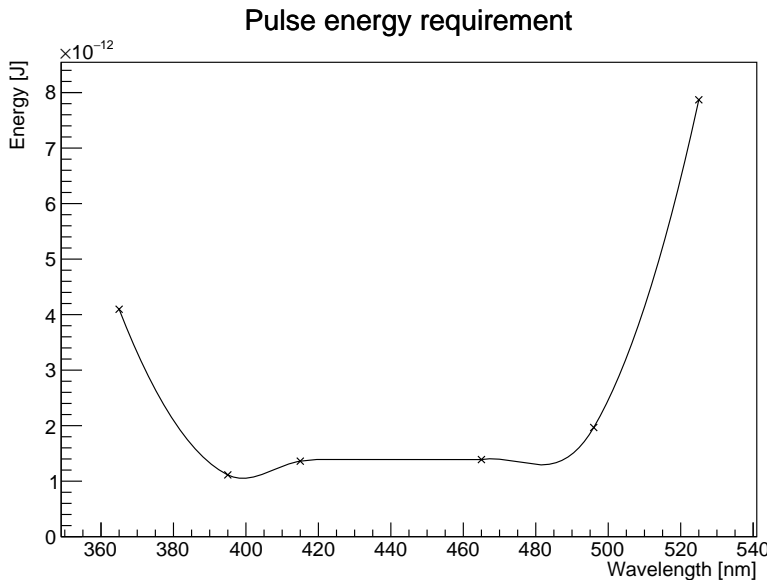


Figure 24: Laser pulse energy as a function of wavelength required to achieve 1% diffuser spot coverage.

these numbers are considered conservative, and the final efficiency of the device will depend on the internal fibre used. Finally, a factor of 50% is included to account for any losses in coupling fibres together across the system.

Applying these scaling factors to the requirements in Table XV yields the required number of photons per pulse from the laser, which goes up to at most 2.4×10^5 at 525 nm. This can easily be translated to the required energy per pulse, which is given in Figure 24. Finally, assuming a 1 kHz pulse frequency for occasional intensive calibration runs, the average power required of the lasers at each wavelength is given in Figure 25.

9 Summary

This technical note describes the tests performed on candidate fibre optic cables, which are used to justify the choices made for optimal fibres to use for the ID and OD systems. For the ID system, along with the OD collimators, Thorlabs FG105UCA is chosen. This fibre showed the least attenuation of the four types tested, in the UV wavelength range which is of most interest, and also matches the fibre type that has already been chosen as the internal feed-through for the optics themselves. This reduces losses that would otherwise be obtained when coupling fibres of

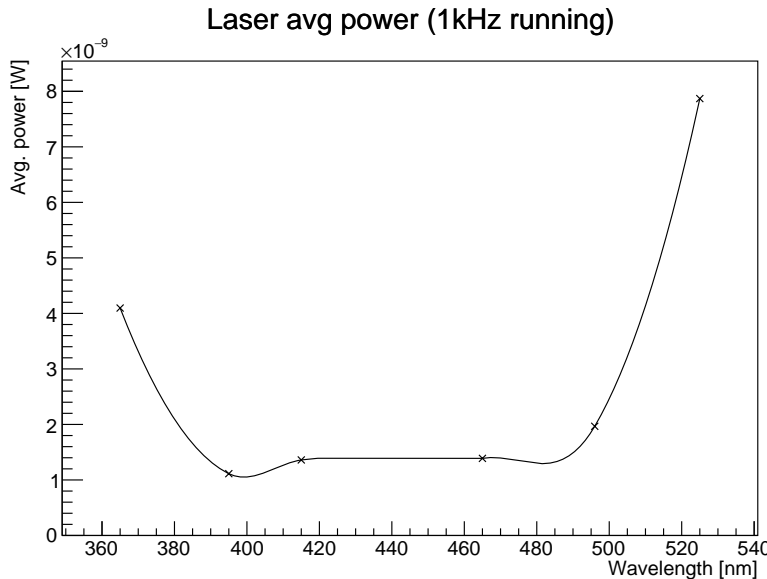


Figure 25: Laser average power as a function of wavelength required to achieve 1% diffuser spot coverage, for 1 kHz running.

800 different types together. This is the reason for choosing this fibre, despite the fact it exhibits a
 801 greater increase in pulse rise time than the other candidates. A high frequency read-out system is
 802 currently in development in order to make complete measurements of the dispersion from the full
 803 lengths of this fibre, as this is still an important property to understand.

804 For the OD diffuser system, the fibre if choice is instead Thorlabs FP400URT. While this
 805 showed increased attenuation at lower wavelengths when compared to FG105UCA, the advantage
 806 of the former fibre type is the diameter being four times greater. This makes coupling an LED to
 807 the fibre considerably easier, and ensures a greater amount of light is directed into the fibre in the
 808 first place.

809 A series of measurements of 1x4 fibre switching devices have also been presented, manufactured
 810 by two different companies. The results for power transmission found the Weinert device with
 811 GIF50C internal fibre to be the best, while for power variation the Agiltron FP400URT device
 812 performed slightly better than the others. However, when making power measurements, none-
 813 zero power measurements were observed on channels of the Agiltron device that were not being
 814 illuminated. Dedicated measurements of this showed cross talk between several different channels
 815 on the Agiltron device, whereas no measurable cross talk was found for either of the Weinert
 816 devices. Coupled with the fact the support from Weinert was vastly superior, which will be
 817 incredibly important for maintaining the device over the lifetime of the experiment, the favoured
 818 company is Weinert. The internal fibre will be the same as that used for the ID laser system, and
 819 as such should be FG105UCA, as discussed already.

820 References

- 821 [1] S. Boyd *et al.*, Hyper-Kamiokande Light Injector Diffuser Technical Note (HK-TN-0042)
- 822 [2] S. Boyd *et al.*, Hyper-Kamiokande Light Injector Collimator Technical Note (HK-TN-0065)
- 823 [3] PicoQuant GmbH, PicoQuant, <https://www.picoquant.com>
- 824 [4] PicoQuant GmbH, Sepia PDL 828 Multichannel Picosecond Diode Laser Driver, September
825 2021, https://www.picoquant.com/images/uploads/downloads/7920-sepia_pdl828.pdf
- 826 [5] PicoQuant GmbH, LDH Series Picosecond Laser Diode Heads for PDL 800-D/PDL 828,
827 January 2024, https://www.picoquant.com/images/uploads/downloads/datasheet_ldh_series.pdf
- 828 [6] PicoQuant GmbH, LDH-FA Series Amplified Picosecond Pulsed Laser Diode Heads, September
829 2022, https://www.picoquant.com/images/uploads/downloads/18-ldh-fa-series_3.pdf
- 830 [7] Thorlabs Inc., FP200URT Specifications, 6th February 2024, <https://www.thorlabs.com/drawings/d13a8cb83b2fa5fc-1B09855E-D596-03E0-87CB959C07E1E119/FP200URT-SpecSheet.pdf>
- 831 [8] Thorlabs Inc., FP400URT Specifications, 6th December 2022, <https://www.thorlabs.com/drawings/d13a8cb83b2fa5fc-1B09855E-D596-03E0-87CB959C07E1E119/FP400URT-SpecSheet.pdf>
- 832 [9] Thorlabs Inc., FG050UGA Specifications, 22nd April 2024, <https://www.thorlabs.com/drawings/d13a8cb83b2fa5fc-1B09855E-D596-03E0-87CB959C07E1E119/FG050UGA-SpecSheet.pdf>
- 833 [10] Thorlabs Inc., FG105UCA Specifications, 22nd April 2024, <https://www.thorlabs.com/drawings/d13a8cb83b2fa5fc-1B09855E-D596-03E0-87CB959C07E1E119/FG105UCA-SpecSheet.pdf>
- 834 [11] Thorlabs Inc., GIF50C Specifications, 6th February 2024, <https://www.thorlabs.com/drawings/d13a8cb83b2fa5fc-1B09855E-D596-03E0-87CB959C07E1E119/GIF50C-SpecSheet.pdf>
- 835 [12] Thorlabs Inc., GIF50D Specifications, 6th February 2024, <https://www.thorlabs.com/drawings/d13a8cb83b2fa5fc-1B09855E-D596-03E0-87CB959C07E1E119/GIF50D-SpecSheet.pdf>
- 836 [13] Thorlabs Inc., Optical Power Meter PM100USB Operation Manual v1.7, 28th March 2023, <https://www.thorlabs.com/drawings/358f9a4c347897ec-F6D46DF6-F3B1-0FC2-1D78C79FC5065F04/PM100USB-Manual.pdf>
- 837 [14] Thorlabs Inc., Fiber Power Head with Silicon Detector S150C, 4th February 2016, <https://www.thorlabs.com/drawings/d13a8cb83b2fa5fc-1B09855E-D596-03E0-87CB959C07E1E119/S150C-SpecSheet.pdf>

- 856 [15] Hamamatsu Photonics K.K., Photomultiplier Tube Modules H10720/H10721 Series,
857 September 2024, https://www.hamamatsu.com/content/dam/hamamatsu-photonics/sites/documents/99_SALES_LIBRARY/etd/H10720_H10721 TPM01062E.pdf
- 859 [16] Tektronix Inc., 5 Series MSO Mixed Signal Oscilloscope Datasheet, <https://www.tek.com/en/datasheet/5-series-mso>
- 861 [17] Y. Nishimura, The Box-and-Line PMT (R12860), (HK-TN-0009 Ver.1.2 RevId20200718)
- 862 [18] Thorlabs Inc., ADAFC1 - FC/PC to FC/PC Mating Sleeve,
863 Wide Key (2.2 mm), D-Hole, <https://www.thorlabs.com/drawings/2a489cabfd9515d-9C4A02B3-EAE7-54D1-C7D705D1F6B147AD/AD AFC1-SpecSheet.pdf>
- 865 [19] K. Abe *et al.*, Second gadolinium loading to Super-Kamiokande, NIM A 1065 (2024), <https://doi.org/10.1016/j.nima.2024.169480>
- 867 [20] Agiltron, <https://agiltron.com>
- 868 [21] Weinert Industries, <https://weinert-industries.com/en/>
- 869 [22] Far Facility Working Group, Water tank and PMT support structure (HK-TN-0048)
- 870 [23] WCSim, <https://github.com/WCSim/WCSim>

871 **A Additional Cross Talk Plots**

872 **A.1 Weinert FP400URT**

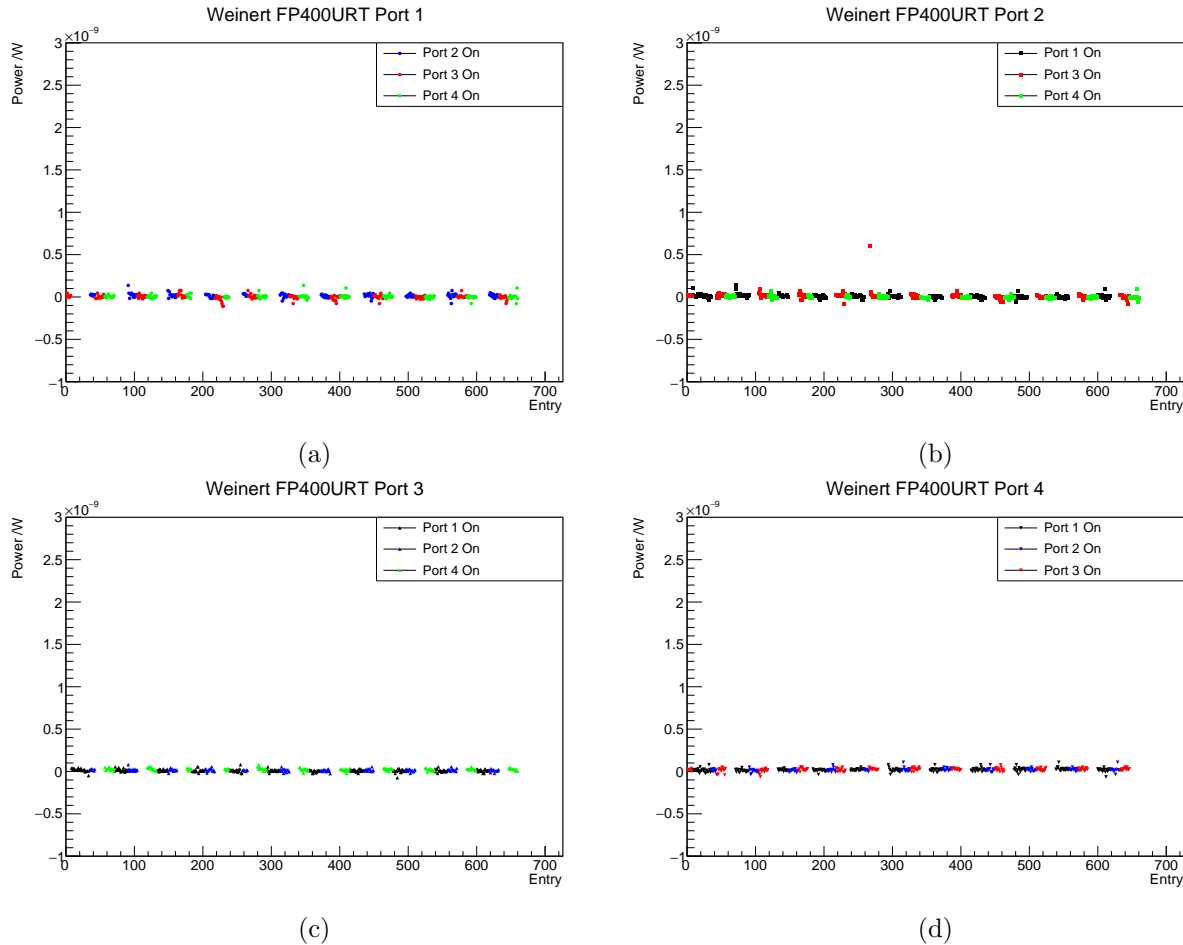


Figure 26: Power recorded on a) port 1, b) port 2, c) port 3 and d) port 4 of the Weinert FP400URT switch, when one of the other three ports was illuminated.

873 A.2 Weinert GIF50C

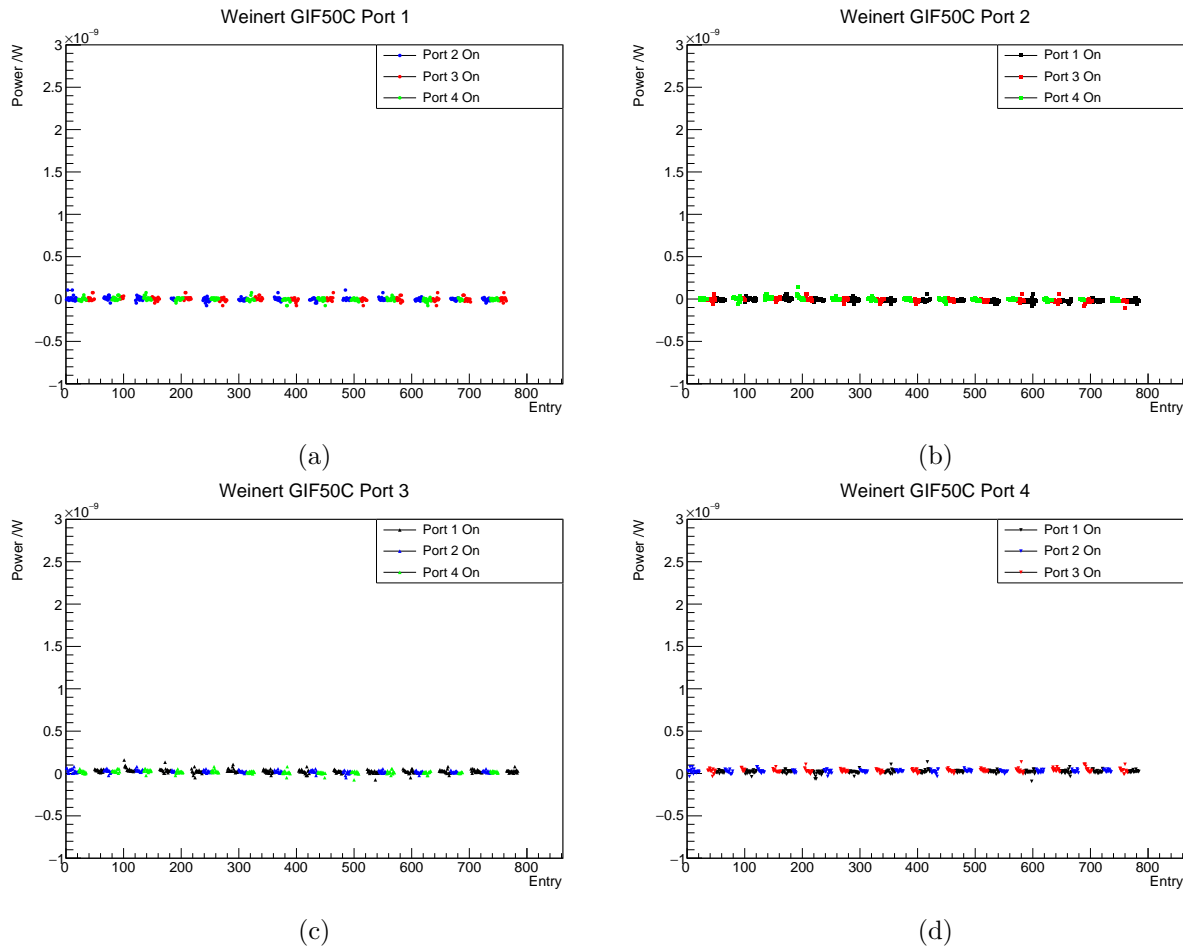


Figure 27: Power recorded on a) port 1, b) port 2, c) port 3 and d) port 4 of the Weinert GIF50C switch, when one of the other three ports was illuminated.